

Heavy quarkonium moving in a hot and dense deconfined nuclear matter

Lata Thakur,^{1,*} Najmul Haque,^{2,†} and Hiranmaya Mishra^{1,‡}

¹*Theory Division, Physical Research Laboratory, Navrangpura, Ahmedabad 380 009, India*

²*Institut für Theoretische Physik, Justus-Liebig-Universität Giessen,
35392 Giessen, Germany*

We study the behavior of the complex potential between a heavy quark and its anti-quark, which are in relative motion with respect to a hot and dense medium. The heavy quark-antiquark complex potential is obtained by correcting both the Coulombic and the linear terms in the Cornell potential through a dielectric function estimated within real-time formalism using the hard thermal loop (HTL) approximation. We show the variation of both the real and the imaginary parts of the potential for different values of velocities when the bound state ($Q\bar{Q}$ pair) is aligned in the direction parallel as well as perpendicular to the relative velocity of the $Q\bar{Q}$ pair with the thermal medium. With increase of the relative velocity the screening of the real part of potential becomes weaker at short distances and stronger at large distances for the parallel case. However, for the perpendicular case, the potential decreases with increase in velocity at all the distances which results in the larger screening of the potential. In addition, the inclusion of the string term makes the screening of the potential weaker as compared to the Coulombic term alone for both the cases. Therefore, combining all these effects we expect a stronger binding of a $Q\bar{Q}$ pair in moving medium in the presence of the string term as compared to the Coulombic term alone. The imaginary part decreases (in magnitude) with increase in the relative velocity leading to a decrease in the width of the quarkonium state at higher velocities. Inclusion of the string term increases the magnitude of imaginary part which results to increase the width of the quarkonium states. All of these effects lead to the modification in the dissolution of quarkonium states.

PACS numbers: 11.10.Wx, 14.40.Pq, 12.38.Bx, 12.38.Mh

Keywords: Heavy quarkonium, Heavy quark-antiquark potential, Dielectric permittivity, Thermal width, Debye mass, String tension.

* latathakur@prl.res.in

† Najmul.Haque@theo.physik.uni-giessen.de

‡ hm@prl.res.in

I. INTRODUCTION

The heavy quarks (HQs) produced in the early stage of the relativistic heavy-ion-collisions are the great interest in investigating the properties of the Quark Gluon Plasma (QGP). HQs can travel through the thermalized QGP medium, and can retain the information about the interaction with them very efficiently. In QGP medium, plasma screening effect are expected to modify the heavy quark-antiquark ($Q\bar{Q}$) potential and above a certain threshold temperature this may lead to a dissolution of $Q\bar{Q}$ bound states [1, 2]. As the low-lying heavy quarkonium $Q\bar{Q}$ bound states are the only hadronic states that can survive in the deconfined phase [3, 4], they are considered as the most powerful probes. Quarkonium suppression can be used to test the formation of a QGP in ultra-relativistic heavy-ion-collisions. In the recent years the quarkonium spectral functions and meson current correlators have been studied using both analytic potential models [5–12] and numerical lattice QCD model [13–22]. Additionally, the theoretical study of quarkonia in a thermal medium was also formulated in the language of effective field theory (EFT) where a sequence of EFTs [23–27] are derived by considering small velocity of the heavy quark and it produces a hierarchy of scales of the heavy quark bound state: $m_Q v^2 \ll m_Q v \ll m_Q$. These hierarchy of scales in EFT makes the analysis complicated and lattice techniques are needed to test the approach. Moreover, the numerical lattice QCD study the quarkonium suppression by calculating spectral functions which are reconstructed from the Euclidean correlators constructed on the lattice. However, lattice QCD can not be used directly to reconstruct the spectral functions from the quarkonium correlators as it is difficult to perform an analytic continuation from imaginary to real time. Another important theoretical finding in this context was the appearance of a complex potential at finite temperature [28], which has stimulated further the imaginary potential model studies [29, 30] as well as attempts to obtain the imaginary potential from the lattice QCD [31, 32]. Earlier it was thought that $Q\bar{Q}$ states dissociate when the Debye screening of the color charge becomes so strong that it prevents the formation of bound states [1]. In recent years the new suggestion is that the quarkonium states dissociate at a lower temperature [28, 33], when the binding energy of the quarkonium is non-vanishing but exceeded by the thermal width [28] which is induced by the Landau-damping and the thermal width can be obtained [28, 34, 35] from the imaginary part of the $Q\bar{Q}$ potential. The importance of the imaginary part of the potential has also been pointed out in recent perturbative calculations [28, 33] that the corresponding thermal width (Γ) of the $Q\bar{Q}$ bound states determines dissociation temperature of the bound state. The imaginary part of the potential has been used earlier to construct the quarkonium spectral functions [29, 33] and also to calculate the perturbative thermal widths [34, 36]. Additionally, it has also been used to study the quarkonium properties using T-matrix approach [3, 37–40], and using stochastic real-time dynamics [41].

In recent years there has been a renewed interest in the properties of bound states moving in a thermal medium due to the advent of high energy heavy-ion colliders. The first study of single heavy quark potential and also the real part of the potential between heavy quark and heavy antiquark pair moving with respect to the QGP was calculated in [42] using a kinetic theory approach. Later, the screening potential of a single moving heavy quark has also been calculated by using semi-classical transport theory in [43]. Later the formation of wakes created by a heavy moving parton in the QGP has also been studied [44–48]. The propagation of non-relativistic bound states moving at constant velocity across a homogeneous thermal bath has been studied in [49], in which the effective field theory (EFT) has been developed, which is relevant in various dynamical regimes. Ref. [49] have studied for the first time the imaginary part of the potential between a quark and antiquark moving in a thermal bath. Later the decay width was also calculated from the imaginary part of the potential in [50]. Authors in Ref. [50] have studied the modifications of some properties of weakly coupled heavy quarkonium states propagating through a QGP at temperatures much

smaller than heavy quark mass, m_Q , where the two different hierarchies have been considered. The first hierarchy corresponds to the $m_Q \gg 1/r \gg T \gg E \gg m_D$, relevant for moderate temperatures, where r is the size of the bound state, E the binding energy, T , the temperature, and m_D is the screening mass. The second hierarchy corresponds to $m_Q \gg T \gg 1/r$, $m_D \gg E$, relevant for studying the dissociation mechanism [50]. Recently the thermal width of heavy quarkonia moving with respect to the QGP has been calculated up to the next-to leading order (NLO) in perturbative QCD in [51]. At the leading order (LO), the width decreases with increasing speed, whereas at the NLO, it increases with a magnitude approximately proportional to the expectation value of the relative velocity between the quarkonium and a parton in thermal equilibrium. Additionally, we note that heavy $Q\bar{Q}$ potential in a moving medium from holographic QCD can be found in Refs. [52–60]. But whether AdS/CFT calculations represent real QCD phenomena or not, that fact still remain controversial. Therefore we follow the weak coupling technique to calculate the complex potential and decay width of a quarkonium in a moving QGP medium.

Most of the analytic calculations that are available in the literature [49, 50, 61–63] using perturbative approaches to calculate the real as well as the imaginary part of the heavy quark-antiquark potential have been done only by considering the thermal modification of vacuum Coulomb potential. Numerical lattice calculations have suggested that the transition from confined nuclear matter to deconfined matter is a crossover [64], rather than a phase transition. So, confinement term in the Cornell potential should be non-vanishing even above transition temperature. Moreover, to study the large distance properties which helps to understand the various bulk properties of the QGP medium [65–67], confinement potential term is necessary. So, it is reasonable to study the effect of the string term above the deconfinement temperature [68–70]. Recently, the real [71, 72] and the imaginary parts [73] of the potential have been calculated by modifying both the Coulombic and the linear string terms of the Cornell potential in the static medium.

Most of the calculations have been done so far to study heavy $Q\bar{Q}$ bound state properties is at vanishing chemical potential of the thermal medium. But there are some calculations at non-vanishing chemical potential also both in perturbative and non-perturbative approaches. For example, the color screening effect at both finite temperature and chemical potential has been studied in thermo-field dynamics approach [74, 75] to calculate the Debye screening mass, where authors have used the phenomenological potential model [2] and error function-type confined force with color screened Coulomb-type potential. Lattice QCD has also studied the color screening in heavy quark potential at finite density with Wilson fermions [76], although it has severe limitation at finite chemical potential. Recently properties of quarkonium states has also been studied in a static medium at finite chemical potential [77] perturbatively.

In the present work we study the behavior of the real and the imaginary parts of the potential between a heavy quark and its anti-quark, which is in relative motion with respect to the thermal bath. In order to calculate the complex potential we modify both the perturbative and non-perturbative terms of the vacuum potential through the dielectric function in real-time formalism using the hard thermal loop (HTL) approximation. Each potential term (real or imaginary) depends on the angle between the orientation of the dipole and the direction of motion of the thermal medium. In our calculation we consider two particular cases: (i) when heavy quarkonium state is aligned along and (ii) perpendicular to the direction of the moving thermal medium. We also construct a general expression for the potential at any angle between the orientation of the dipole and the direction of the relative motion of the thermal medium. It is important to discuss that whether the dissociation mechanism (screening versus Landau damping) remains the same when the bound state moves with respect to the thermal bath. Therefore, we calculate the decay width from the imaginary part of the potential in perturbation theory and also show the effect of the string term on it. We also study the chemical potential dependence in the various quantities that we are interested in.

This paper is structured as follows. In section II we introduce general framework about the properties of the moving particles in a deconfined thermal medium. In section III we discuss the self energies and propagators in moving medium. In section IV we discuss the mass prescription of the Debye mass that we use here. In section V we study the medium modified heavy quark potential in a moving thermal bath and also discuss the variation of real and imaginary parts of the potential with various velocities when $Q\bar{Q}$ pair is along and perpendicular to the direction of the velocity of the thermal medium. In section VI we study the thermal decay width and finally we present our conclusion in section VII.

II. GENERAL FRAMEWORK

We consider a reference frame in which the QGP medium moves with a velocity \mathbf{v} and the $Q\bar{Q}$ bound state is at rest. The particle distribution functions can be written as [49]

$$f(\beta^\mu P_\mu) = \frac{1}{e^{|\beta^\mu P_\mu|} \pm 1}, \quad (1)$$

where the $+$ ($-$) sign corresponds to fermions (bosons) and

$$\beta^\mu = \frac{\gamma}{T}(1, \mathbf{v}) = \frac{u^\mu}{T}, \quad (2)$$

where $\gamma = 1/\sqrt{1-v^2}$, $v = |\mathbf{v}|$, is the Lorentz factor. We use the following notation for the four and the three momenta in the above equation and also in the remaining part of the article: $P = (p_0, \mathbf{p})$, $p = |\mathbf{p}|$. The moving plasma frame has been successfully used long ago in [78]. Study of a quakonium in a moving medium is equivalent to study a quakonium in non-equilibrium field theory [79]. In non-equilibrium case the equilibrium Fermi-Dirac or the Bose-Einstein distribution functions are replaced by non-equilibrium distribution functions, whereas in the case of moving thermal medium distribution functions will be the boosted Fermi-Dirac or Bose-Einstein distribution functions Eq. (1). In the non-equilibrium field theory we can write [49]

$$\beta^\mu P_\mu = p \frac{1 - v \cos \theta}{T\sqrt{1-v^2}}, \quad (3)$$

where θ is the angle between \mathbf{p} and \mathbf{v} . The distribution functions (Eq. 1) can be written as

$$f(p, T, \theta, v) = \frac{1}{e^{p/T_{\text{eff}}(\theta, v)} \pm 1}, \quad (4)$$

where the *effective temperature* can be defined as

$$T_{\text{eff}}(\theta, v) = \frac{T\sqrt{1-v^2}}{1 - v \cos \theta}. \quad (5)$$

The dependency on v and θ in the effective temperature can be understood as a Doppler effect. For small values of v ($v \ll 1$), $T_{\text{eff}}(\theta, v) \sim T$ and the Boltzmann factor in Eq. (4) does not depend on angle θ , rather depends only one scale T . On the other hand, when v is close to unity, the values of $T_{\text{eff}}(\theta, v)$ depend on θ . The number of scale introduced by moving thermal medium can be understood by using light cone co-ordinates [49, 50]. In light cone co-ordinates the distribution function depends upon two scales i.e. T_+ and T_- . Here we consider both the scales T_+ and T_- of same order of magnitude as considered in Ref. [50].

III. SELF ENERGIES AND PROPAGATORS

To study the effect of the moving medium on the properties of the quarkonium states, one needs to calculate first the self energies and propagators in a moving medium. We can calculate the self energies and propagators in real-time formalism [79] in the HTL approximation by assuming that the temperature of the plasma is $T \gg 1/r$. As we shall see in section V, the heavy quark-antiquark potential is the Fourier transform of the physical 11 component of the gluon propagator in real time formalism in the static limit. So, the “11” component of the longitudinal gluon propagator can be written in terms of the retarded (D_R), advanced (D_A) and symmetric (D_S) propagators in the real time formalism in static limit as

$$D_{11}^L(p_0 = 0, \mathbf{p}) = \frac{1}{2} [D_R^L(\mathbf{p}) + D_A^L(\mathbf{p}) + D_S^L(\mathbf{p})] . \quad (6)$$

The retarded (advanced) propagator can be obtained from the retarded (advanced) self energy and symmetric propagator can be obtained from the symmetric self energy. For the bound state moving through the thermal bath, the symmetric propagator [49] can be written as

$$D_S^L(\mathbf{p}, u) = \frac{\Pi_S^L(\mathbf{p}, u)}{2i\Im\Pi_R^L(\mathbf{p}, u)} [D_R^L(\mathbf{p}, u) - D_A^L(\mathbf{p}, u)] , \quad (7)$$

where $u^\mu = \gamma(1, \mathbf{v})$ is the 4-velocity and \Re and \Im represent the real and imaginary parts respectively. $D_R(\mathbf{p}, u)$ ($D_A(\mathbf{p}, u)$) represents the retarded (advanced) propagator for the bound state moving through the thermal bath. In order to determine the propagator one has to evaluate the self-energies $\Pi_R(\mathbf{p}, u)$ and $\Pi_S(\mathbf{p}, u)$. The retarded self-energy $\Pi_R(\mathbf{p}, u)$ was computed in [42] and later on in Ref. [49] for the reference frame where the bound state is at rest and can be written as

$$\Pi_R(\mathbf{p}, u) = \Pi_R^L(\mathbf{p}, u) = a(z) + \frac{b(z)}{1 - v^2} , \quad (8)$$

where

$$a(z) = \frac{m_D^2}{2} \left[z^2 - (z^2 - 1) \frac{z}{2} \log \left(\frac{z + 1 + i\epsilon}{z - 1 + i\epsilon} \right) \right] , \quad (9)$$

and

$$b(z) = (z^2 - 1) \left[a(z) - m_D^2(1 - z^2) \left\{ 1 - \frac{z}{2} \log \left(\frac{z + 1 + i\epsilon}{z - 1 + i\epsilon} \right) \right\} \right] , \quad (10)$$

with

$$z = \left| \frac{P \cdot u}{\sqrt{(P \cdot u)^2 - P^2}} \right|_{\omega=0} . \quad (11)$$

We always consider the dipole is aligned along Z-direction. If the velocity is in the parallel direction with the axis of the dipole, then Eq. (11) can be written as

$$z_{\parallel} = \frac{v \cos \theta}{\sqrt{1 - v^2 \sin^2 \theta}} , \quad (12)$$

where (θ, ϕ) represent polar and azimuthal angles of momentum vector respectively. Similarly, if the relative velocity of the medium is in XY - plane in the direction which makes an angle β with the X - axis, then Eq. (11) can be written as

$$z_{\perp} = \frac{v \sin(\theta) \cos(\phi - \beta)}{\sqrt{1 - v^2 - v^2 \sin^2 \theta \cos^2(\phi - \beta)}} . \quad (13)$$

Using Eq. (8) - Eq. (13), the retarded gluon self energy in the above mentioned two directions can be written as

$$\Pi_R^{\parallel}(\theta, v) = \frac{m_D^2}{2} \left[\frac{2 - 2v^2 - v^4 \cos^2 \theta \sin^2 \theta}{(1 - v^2 \sin^2 \theta)^2} - \frac{(2 + v^2 \sin^2 \theta)(1 - v^2)v \cos \theta}{2(1 - v^2 \sin^2 \theta)^{5/2}} \right. \\ \left. \times \log \left(\frac{v \cos \theta + \sqrt{1 - v^2 \sin^2 \theta}}{v \cos \theta - \sqrt{1 - v^2 \sin^2 \theta}} \right) \right], \quad (14)$$

and

$$\Pi_R^{\perp}(\theta, \phi, \beta, v) = \frac{m_D^2}{2} \left[\frac{2 - 2v^2 - v^4 \cos^2(\phi - \beta) \sin^2 \theta (1 - \cos^2(\phi - \beta) \sin^2 \theta)}{(1 - v^2 + v^2 \cos^2(\phi - \beta) \sin^2 \theta)^2} \right. \\ \left. - \frac{(2 + v^2 - v^2 \cos^2(\phi - \beta) \sin^2 \theta)(1 - v^2)v \cos(\phi - \beta) \sin \theta}{2(1 - v^2 + v^2 \cos^2(\phi - \beta) \sin^2 \theta)^{5/2}} \right. \\ \left. \times \log \left(\frac{v \cos(\phi - \beta) \sin \theta + \sqrt{1 - v^2 + v^2 \cos^2(\phi - \beta) \sin^2 \theta}}{v \cos(\phi - \beta) \sin \theta - \sqrt{1 - v^2 + v^2 \cos^2(\phi - \beta) \sin^2 \theta}} \right) \right], \quad (15)$$

where m_D represent Debye mass.

Using the retarded self energy one can obtain the retarded propagator as

$$D_R^{\parallel(\perp)}(\mathbf{p}, u) = D_R^{L, \parallel(\perp)}(\mathbf{p}, u) \frac{1}{p^2 + \Pi_R^{\parallel(\perp)}(\mathbf{p}, u)}. \quad (16)$$

For a bound state in the moving thermal bath, it is enough to calculate the retarded self energy and the advanced self energy can be obtained from the relation $D_R^{*\parallel(\perp)}(\mathbf{p}, u) = D_A^{\parallel(\perp)}(\mathbf{p}, u)$. Similarly, one can calculate the symmetric self energy for both the cases as

$$\Pi_S^{\parallel}(\mathbf{p}, u) = \Pi_S^{L, \parallel} = \Pi_1 + \frac{\Pi_2}{1 - v^2} = \frac{i2\pi m_D^2 T(1 - v^2)^{3/2} \left(1 + \frac{v^2}{2} \sin^2 \theta\right)}{|\mathbf{p}| (1 - v^2 \sin^2 \theta)^{5/2}}. \quad (17)$$

and

$$\Pi_S^{\perp}(\mathbf{p}, u) = \Pi_S^{L, \perp} = \Pi_1 + \frac{\Pi_2}{1 - v^2} = \frac{i2\pi m_D^2 T(1 - v^2)^{3/2} \left(1 + \frac{v^2}{2} - \frac{v^2}{2} \cos^2(\phi - \beta) \sin^2 \theta\right)}{|\mathbf{p}| (1 - v^2 + v^2 \cos^2(\phi - \beta) \sin^2 \theta)^{5/2}}. \quad (18)$$

Symmetric propagator $D_S^L(\mathbf{p}, u)$ can be obtained by substituting the symmetric self energy in Eq. (7) as

$$D_S^{\parallel(\perp)}(\mathbf{p}, u) = \frac{\Pi_S^{\parallel(\perp)}(\mathbf{p}, u)}{2i\Im \Pi_R^{\parallel(\perp)}(\mathbf{p}, u)} \left(D_R^{\parallel(\perp)}(\mathbf{p}, u) - D_A^{\parallel(\perp)}(\mathbf{p}, u) \right), \quad (19)$$

As $D_A(\mathbf{p}, u) = D_R^*(\mathbf{p}, u)$, so $D_R(\mathbf{p}, u) - D_A(\mathbf{p}, u)$ can be written as

$$D_R^{\parallel(\perp)}(\mathbf{p}, u) - D_A^{\parallel(\perp)}(\mathbf{p}, u) = \frac{1}{p^2 + \Pi_R^{\parallel(\perp)}(\mathbf{p}, u)} - \frac{1}{p^2 + \Pi_R^{*\parallel(\perp)}(\mathbf{p}, u)} \\ = \frac{2i\Im \Pi_R^{\parallel(\perp)}(\mathbf{p}, u)}{\left(p^2 + \Pi_R^{\parallel(\perp)}(\mathbf{p}, u) \right) \left(p^2 + \Pi_R^{*\parallel(\perp)}(\mathbf{p}, u) \right)}. \quad (20)$$

Therefore we get the symmetric propagator for the parallel case as

$$D_S^{\parallel}(\mathbf{p}, u) = D_S^{L, \parallel}(\mathbf{p}, u) = \frac{-2\pi i m_D^2 T (1 - v^2)^{3/2} (2 + v^2 \sin^2 \theta)}{2p (1 - v^2 \sin^2 \theta)^{5/2} \left(p^2 + \Pi_R^{\parallel}(\mathbf{p}, u) \right) \left(p^2 + \Pi_R^{*\parallel}(\mathbf{p}, u) \right)} \quad (21)$$

and for the perpendicular case as

$$D_S^{\perp}(\mathbf{p}, u) = D_S^{L, \perp}(\mathbf{p}, u) = \frac{-2\pi i m_D^2 T (1 - v^2)^{3/2} (2 + v^2 - v^2 \cos^2(\phi - \beta) \sin^2 \theta)}{2p (1 - v^2 + v^2 \cos^2(\phi - \beta) \sin^2 \theta)^{5/2} \left(p^2 + \Pi_R^{\perp}(\mathbf{p}, u) \right) \left(p^2 + \Pi_R^{*\perp}(\mathbf{p}, u) \right)} \quad (22)$$

Using these above expressions for the self energies and propagators, we calculate the heavy quark potential in a moving medium in the further section.

IV. MASS PRESCRIPTION

We use NLO Debye mass as given in [80] and the expression of m_D^2 can be written at finite chemical potential ($\mu \neq 0$) as

$$\begin{aligned} m_D^2 = & \frac{4\pi\alpha_s}{3} T^2 \left[N_c + \frac{N_c^2 \alpha_s}{12\pi} \left(5 + 22\gamma_E + 22 \ln \frac{\Lambda}{4\pi T} \right) + \frac{N_f}{2} (1 + 12\hat{\mu}^2) \right. \\ & + \frac{N_c N_f \alpha_s}{24\pi} \left\{ (9 + 132\hat{\mu}^2) + 22 (1 + 12\hat{\mu}^2) \gamma_E + 2 (7 + 132\hat{\mu}^2) \ln \frac{\Lambda}{4\pi T} + 4\aleph(\hat{\mu}) \right\} \\ & \left. + \frac{N_f^2 \alpha_s}{12\pi} (1 + 12\hat{\mu}^2) \left(1 - 2 \ln \frac{\Lambda}{4\pi T} + \aleph(\hat{\mu}) \right) - \frac{3}{8\pi} \frac{N_f (N_c^2 - 1) \alpha_s}{N_c} (1 + 12\hat{\mu}^2) \right], \quad (23) \end{aligned}$$

where N_c represents number of colors, N_f represents number of flavors, $\hat{\mu} = \mu/(2\pi T)$, $\aleph(\hat{\mu}) = \psi(1/2 - i\hat{\mu}) + \psi(1/2 + i\hat{\mu})$, ψ denotes digamma function. The expression for running coupling α_s in one loop level can be written as

$$\alpha_s = \frac{12\pi}{11N_c - 2N_f} \frac{1}{\ln(\Lambda^2/\Lambda_{\overline{\text{MS}}}^2)}. \quad (24)$$

We use $\Lambda_{\overline{\text{MS}}} = 176$ MeV and renormalization scale $\Lambda = 2\pi\sqrt{T^2 + \mu^2/\pi^2}$ as discussed in [80]. We want to mention here that, if one uses higher order running coupling, the value of α_s and m_D would remain the same. In those case, only the values of $\Lambda_{\overline{\text{MS}}}$ will get modified.

The quantities that we discuss in this article depend on the quark chemical potential only via the Debye mass. In most of the numerical plots, we take vanishing chemical potential. But in some cases we also take finite chemical potential. Whenever there is finite value of the chemical potential, we mention it. If the value of μ is not mentioned, it implies vanishing chemical potential.

V. HEAVY QUARK-ANTIQUARK POTENTIAL IN A MOVING MEDIUM

In the present section we study the modification of the Cornell potential of a heavy quark-antiquark which is in relative motion with respect to the thermal bath. We evaluate the potential

in the HTL approximation by assuming that the temperature of the plasma is $T \gg 1/r$. Medium-modification to the vacuum potential can be obtained by correcting both perturbative (short-distance) and non-perturbative (long-distance) parts with a dielectric function $\epsilon(p)$ encoding the effect of deconfinement [71, 72]

$$V(\mathbf{r}, T, \mathbf{v}) = \int \frac{d^3\mathbf{p}}{(2\pi)^{3/2}} (e^{i\mathbf{p}\cdot\mathbf{r}} - 1) \frac{V(p)}{\epsilon(p, u)}, \quad (25)$$

where r -independent term (perturbative free energy term of a quarkonium at infinite separation [61]) has been subtracted to renormalize the heavy quark free energy. $V(p)$ is the Fourier transforms (FT) of the Cornell potential which can be written from Ref. [71] as

$$\begin{aligned} V(p) &= -\sqrt{(2/\pi)} \frac{\alpha}{p^2} - \frac{4\sigma}{\sqrt{2\pi}p^4} \\ &= -\sqrt{(2/\pi)} \frac{C_F\alpha_s}{p^2} - \frac{4\sigma}{\sqrt{2\pi}p^4}, \end{aligned} \quad (26)$$

where $\alpha \equiv C_F\alpha_s$, with $C_F = (N_c^2 - 1)/2N_c$. The dielectric permittivity $\epsilon(\mathbf{p}, u)$ can be obtained from the relation [81]

$$\epsilon^{-1}(\mathbf{p}, u) = \lim_{\omega \rightarrow 0} p^2 D_{11}^L(\omega, \mathbf{p}, u), \quad (27)$$

where D_{11}^L is the longitudinal gluon propagator, which can be written in terms of the real and the imaginary parts as

$$D_{11}^L(\mathbf{p}, u) = \Re D_{11}^L(\mathbf{p}, u) + \Im D_{11}^L(\mathbf{p}, u), \quad (28)$$

The real part of the propagator can be written in terms of the retarded and advanced propagators and also the imaginary part can be written in terms of the symmetric propagator as

$$\Re D_{11}^L(\mathbf{p}, u) = \frac{1}{2} (D_R^L(\mathbf{p}, u) + D_A^L(\mathbf{p}, u)) \text{ and } \Im D_{11}^L(\mathbf{p}, u) = \frac{1}{2} D_S^L(\mathbf{p}, u). \quad (29)$$

Thus using the real and the imaginary parts of propagator we can calculate the real and the imaginary parts of the heavy quark potential as

$$\begin{aligned} V(\mathbf{r}, T, \mathbf{v}) &= \int \frac{d^3\mathbf{p}}{(2\pi)^{3/2}} (e^{i\mathbf{p}\cdot\mathbf{r}} - 1) V(p) p^2 D_{11}^L(\mathbf{p}, u) \\ &= \int \frac{d^3\mathbf{p}}{(2\pi)^{3/2}} (e^{i\mathbf{p}\cdot\mathbf{r}} - 1) V(p) \frac{p^2}{2} (D_R^L(\mathbf{p}, u) + D_A^L(\mathbf{p}, u) + D_S^L(\mathbf{p}, u)). \end{aligned} \quad (30)$$

Eq. (30) can be decomposed into real and the imaginary part of the potential as

$$V(\mathbf{r}, T, \mathbf{v}) = \Re V(\mathbf{r}, T, \mathbf{v}) + \Im V(\mathbf{r}, T, \mathbf{v}), \quad (31)$$

where the real part is

$$\Re V(\mathbf{r}, T, \mathbf{v}) = \int \frac{d^3\mathbf{p}}{(2\pi)^{3/2}} (e^{i\mathbf{p}\cdot\mathbf{r}} - 1) V(p) \frac{p^2}{2} (D_R^L(\mathbf{p}, u) + D_A^L(\mathbf{p}, u)), \quad (32)$$

and the imaginary part is

$$\Im V(\mathbf{r}, T, \mathbf{v}) = \int \frac{d^3\mathbf{p}}{(2\pi)^{3/2}} (e^{i\mathbf{p}\cdot\mathbf{r}} - 1) V(p) \frac{p^2}{2} D_S^L(\mathbf{p}, u). \quad (33)$$

Each potential term (real or imaginary) depends on the angle between the orientation of the dipole and the direction of motion of the thermal medium. For simplicity, we consider two extreme cases *viz.*

- The dipole is aligned parallelly in the direction of relative velocity of the dipole and the medium.
- The dipole is aligned in the perpendicular plane of the direction of relative velocity of the dipole and the medium.

Using the expressions for potential at the parallel and perpendicular alignment, it is possible to construct a general expression for the potential at any angle between orientation of the dipole and the direction of relative motion of the dipole and the medium. We give below the real and the imaginary part of the potential for both the cases.

A. Real part of the potential

The real part of the potential can thus be obtained from Eq. (32) as

$$\begin{aligned}
\Re V(\mathbf{r}, T, \mathbf{v}) &= \int \frac{d^3 \mathbf{p}}{(2\pi)^{3/2}} (e^{i\mathbf{p} \cdot \mathbf{r}} - 1) V(p) \frac{p^2}{2} (D_R^L(\mathbf{p}, u) + D_A^L(\mathbf{p}, u)) \\
&= - \int \frac{d^3 \mathbf{p}}{(2\pi)^{3/2}} (e^{i\mathbf{p} \cdot \mathbf{r}} - 1) \left(\sqrt{(2/\pi)} C_F \alpha_s + \frac{4\sigma}{\sqrt{2\pi} p^2} \right) \Re \left[\frac{1}{p^2 + \Pi_R(\mathbf{p}, u)} \right] \\
&= - \frac{\alpha_s C_F}{r} \\
&\quad - \alpha_s m_D C_F \Re \left[\int_0^{\pi/2} d\theta \sin \theta \left(1 - e^{-m_D r \cos \theta \sqrt{\Pi_R(\theta, v)/m_D^2}} \right) \sqrt{\Pi_R(\theta, v)/m_D^2} \right] \\
&\quad + \frac{\sigma}{2m_D} \Re \left[\int_0^{\pi/2} d\theta \sin \theta \left(1 - e^{-m_D r \cos \theta \sqrt{\Pi_R(\theta, v)/m_D^2}} \right) \frac{1}{\sqrt{\Pi_R(\theta, v)/m_D^2}} \right]. \quad (34)
\end{aligned}$$

When the dipole is aligned parallel to the direction of the relative velocity, real part of the potential can be written as

$$\begin{aligned}
\Re V(\mathbf{r} \parallel \mathbf{v}, T) &= - \frac{\alpha_s C_F}{r} \\
&\quad - \alpha_s m_D C_F \Re \left[\int_0^{\pi/2} d\theta \sin \theta \left(1 - e^{-m_D r \cos \theta \sqrt{\Pi_R^\parallel(\theta, v)/m_D^2}} \right) \sqrt{\Pi_R^\parallel(\theta, v)/m_D^2} \right] \\
&\quad + \frac{\sigma}{2m_D} \Re \left[\int_0^{\pi/2} d\theta \sin \theta \left(1 - e^{-m_D r \cos \theta \sqrt{\Pi_R^\parallel(\theta, v)/m_D^2}} \right) \frac{1}{\sqrt{\Pi_R^\parallel(\theta, v)/m_D^2}} \right]. \quad (35)
\end{aligned}$$

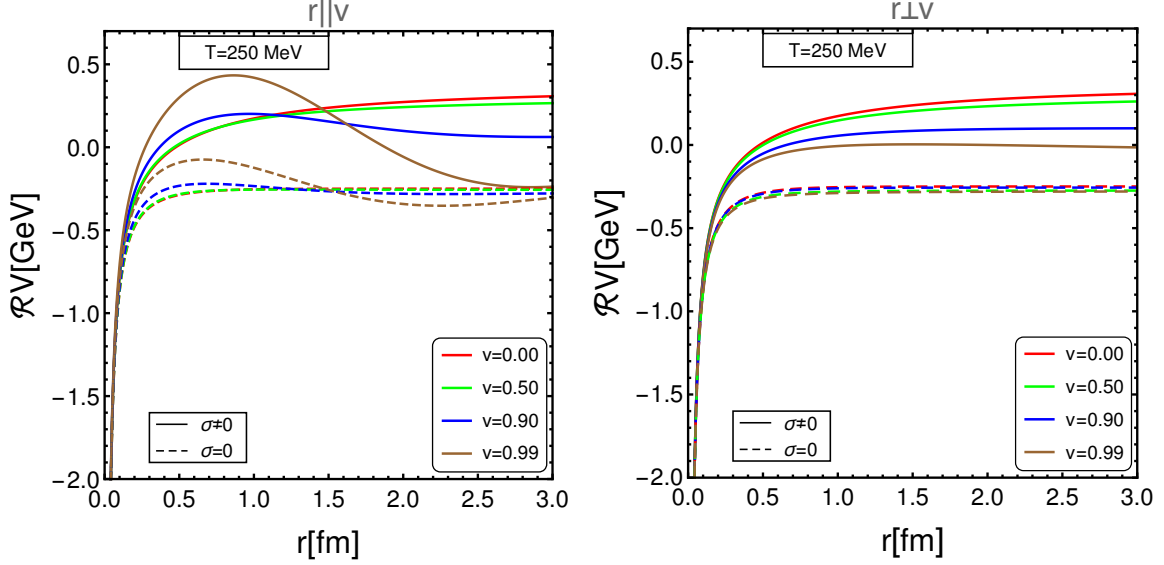


FIG. 1. Variation of the real part of the potential with separation distance r between Q and \bar{Q} for various values of velocity at $T = 250$ MeV when dipole axis is along the velocity direction (left) and perpendicular direction (right) of the thermal medium.

Similarly for the perpendicular case

$$\begin{aligned}
 \Re V(\mathbf{r} \perp \mathbf{v}, T) = & -\frac{\alpha_s m_D C_F}{r} \\
 & - \alpha_s m_D C_F \Re \left[\int_0^{\pi/2} d\theta \sin \theta \int_0^{2\pi} \frac{d\phi}{2\pi} \left(1 - e^{-m_D r \cos \theta \sqrt{\Pi_R^\perp(\theta, \phi, \beta, v)/m_D^2}} \right) \sqrt{\Pi_R^\perp(\theta, \phi, \beta, v)/m_D^2} \right] \\
 & + \frac{\sigma}{2m_D} \Re \left[\int_0^{\pi/2} d\theta \sin \theta \int_0^{2\pi} \frac{d\phi}{2\pi} \left(1 - e^{-m_D r \cos \theta \sqrt{\Pi_R^\perp(\theta, \phi, \beta, v)/m_D^2}} \right) \frac{1}{\sqrt{\Pi_R^\perp(\theta, \phi, \beta, v)/m_D^2}} \right].
 \end{aligned} \tag{36}$$

Fig. 1 shows the variation of the real part of the potential for various values of velocities (*viz.* $v = 0.0, 0.50, 0.90, 0.99$) at $T = 250$ MeV for both the orientation of the dipole. From the figure we find that the real part of the potential increases with increase in velocity at short distances and decreases with increase in velocity at large distances. The increase in velocity makes the real part of the potential less screened at short distances and more screened at large distances for the parallel case. On the other hand, potential decreases with increase in velocity for the perpendicular case which results in more screening of the potential. The inclusion of the string term makes the real part of the potential less screened as compared to the Coulombic term alone for both the cases. Combining all these effects we expect a stronger binding of a $Q\bar{Q}$ pair in the presence of the string term as compared to the Coulombic term alone in the moving medium. Here solid lines represent potential with both coulomb and the string term whereas dashed lines represent the potential in the absence of the non-perturbative (string) term. Real part of the potential shows an oscillation in the ultra-relativistic limit for the parallel case which may be because of the induced dipole interaction in this direction.

Fig. 2 shows the variation of real part of the potential with the separation distance r for different values of temperatures (*viz.* $T = 250$ MeV, 350 MeV, 450 MeV, 550 MeV) for both the parallel and

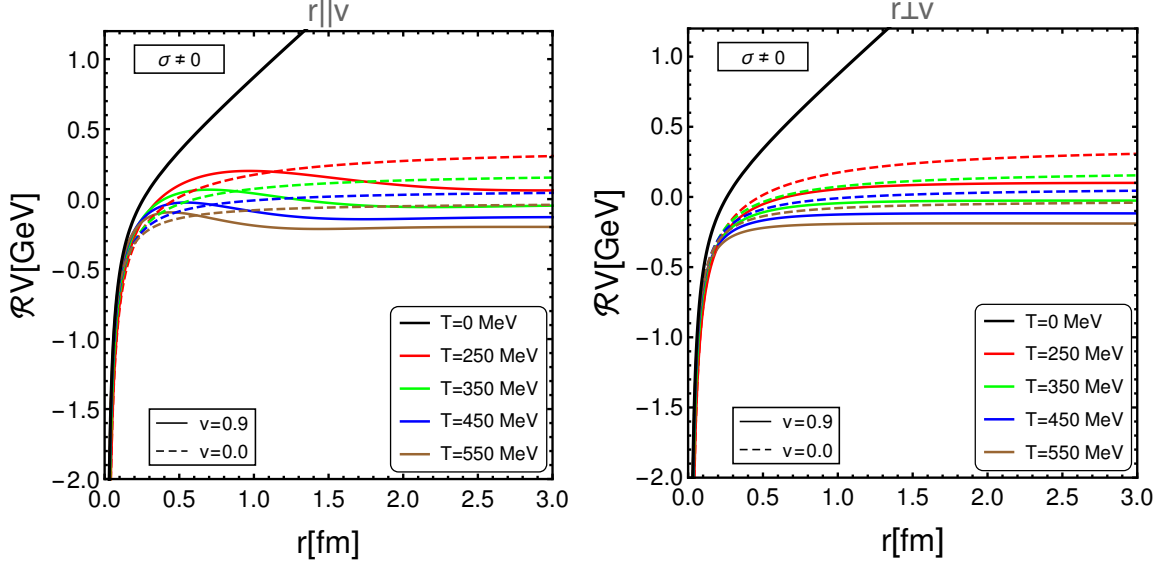


FIG. 2. Variation of the real part of the potential with the separation distance r between Q and \bar{Q} for various values of temperature at $v = 0$ (dotted line) and $v = 0.9$ (solid line) when dipole axis is along the velocity direction (left) and perpendicular direction (right) of the thermal medium along with $T = 0$ (solid black line) potential.

perpendicular cases. In this figure, solid black lines represent $T = 0$ potential. Other solid lines represent potential at $v = 0.9$ and dashed lines represents the potential at $v = 0$. From the figure we find that real part of the potential becomes more screened with increase in temperature for both the cases and becomes short range. Alternatively we can say that at higher temperature $Q\bar{Q}$ state is loosely bound as compared to the lower temperatures. The zero velocity plots in the above two figures quantitatively look similar with the other finite temperature heavy quark-antiquark potential available in literature [5, 65, 82, 83]. Note that the potential does not depend on the angle β . That means the potential is independent on the angle of orientation of the dipole in the XY - plane. In both the figures (Fig. 1 and Fig. 2), we take vanishing chemical potential of the medium.

Fig. 3 shows the variation of real part of the potential with the separation distance r for different values of chemical potential (*viz.* $\mu = 250$ MeV, 350 MeV, 450 MeV, 550 MeV) for both the parallel and perpendicular orientations. We find almost same behavior of the potential with increase in μ as in Fig. 2 with temperature but the potential shows very weak dependence on μ as compared to the temperature (T).

If the angle between dipole axis and the velocity vector is θ_{vr} , then the real part of the potential at any orientation of the dipole can be written as

$$\Re V(\mathbf{r}, T, \mathbf{v}) = \frac{1}{2} \Re V(\mathbf{r} \parallel \mathbf{v}, T) (1 + \cos 2\theta_{vr}) + \frac{1}{2} \Re V(\mathbf{r} \perp \mathbf{v}, T) (1 - \cos 2\theta_{vr}). \quad (37)$$

Fig. 4 shows the variation of real part of potential with the angle, θ_{vr} between the dipole orientation and the velocity direction. We find that real potential remain almost constant with θ_{vr} at small velocities ($v \lesssim 0.55$). It increases at large velocities ($v \gtrsim 0.55$) and decreases with increase in θ_{vr} which is because of the less screening near parallel alignment as compared to near perpendicular alignment. The increase in the value of potential at large velocities is less at high

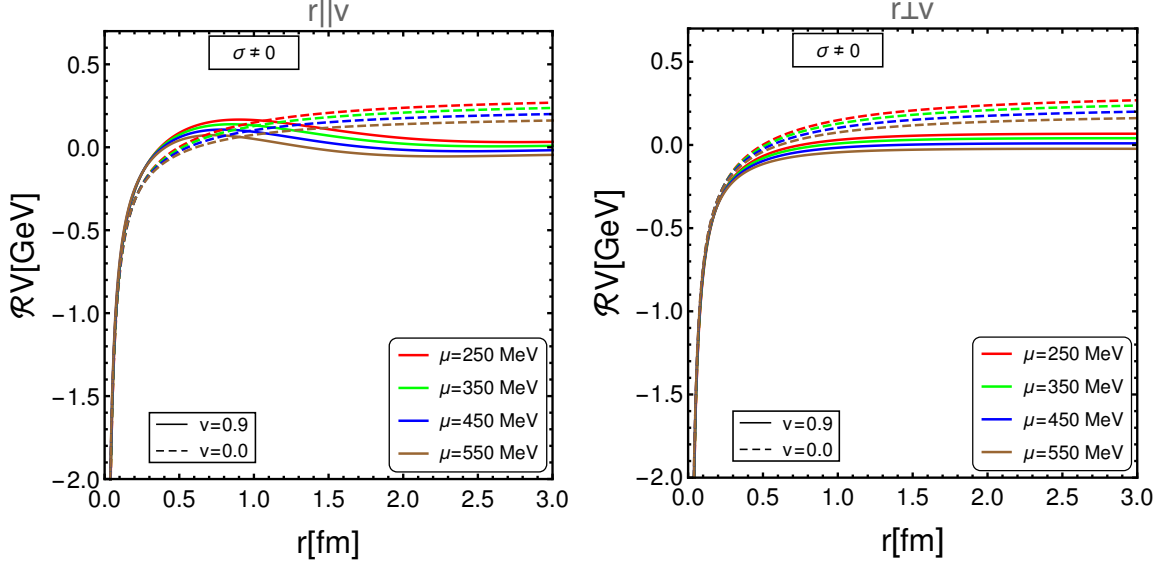


FIG. 3. Variation of the real part of the potential with the separation distance r between Q and \bar{Q} for various values of chemical potential at $v = 0$ (dotted line) and $v = 0.9$ (solid line) when dipole axis is along the velocity direction (left) and the perpendicular direction (right) of the thermal medium.

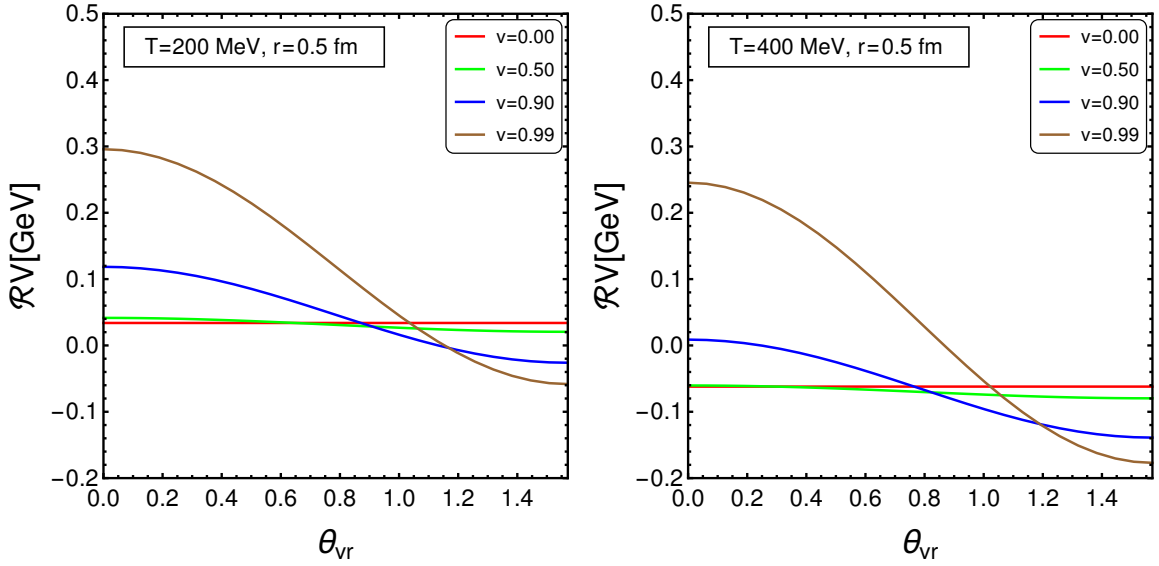


FIG. 4. Real part of the potential for various values of velocity at $T = 200$ MeV (left) and $T = 400$ MeV (right) with the angle θ_{vr} between the dipole orientation and the velocity direction.

temperature ($T = 400$ MeV) as compared to low temperature ($T = 200$ MeV) which is because of more screening at high temperature.

When the relative velocity between the $Q\bar{Q}$ pair and the thermal medium is small ($v \lesssim 0.5$), it is possible to compute the real part of the potential at parallel and perpendicular direction from

Eq. (35) and Eq. (36) respectively in terms of scaled separation $\hat{r}(=rm_D)$ as

$$\begin{aligned} \Re V(\mathbf{r} \parallel \mathbf{v}, T) \approx & -\alpha_s m_D C_F \left[1 + \frac{e^{-\hat{r}}}{\hat{r}} + v^2 \left\{ -\frac{6}{\hat{r}^3} + e^{-\hat{r}} \left(\frac{6}{\hat{r}^3} + \frac{6}{\hat{r}^2} + \frac{3}{\hat{r}} + 1 \right) \right. \right. \\ & + \left. \frac{\pi^2}{2} \left(\frac{1}{\hat{r}^3} + \frac{1}{48} \right) - \frac{e^{-\hat{r}} \pi^2}{2} \left(\frac{1}{\hat{r}^3} + \frac{1}{\hat{r}^2} + \frac{1}{2\hat{r}} + \frac{3}{16} + \frac{\hat{r}}{16} \right) \right\} \Big] \\ & + \frac{2\sigma}{m_D} \left[1 + \frac{e^{-\hat{r}} - 1}{\hat{r}} + v^2 \left\{ -\frac{12}{\hat{r}^3} + \frac{1}{\hat{r}} + e^{-\hat{r}} \left(\frac{12}{\hat{r}^3} + \frac{12}{\hat{r}^2} + \frac{5}{\hat{r}} + 1 \right) \right. \right. \\ & + \left. \left. \frac{\pi^2}{2} \left(\frac{3}{\hat{r}^3} - \frac{1}{16} \right) - \frac{e^{-\hat{r}} \pi^2}{2} \left(\frac{3}{\hat{r}^3} + \frac{3}{\hat{r}^2} + \frac{3}{2\hat{r}} + \frac{7}{16} + \frac{\hat{r}}{16} \right) \right\} \right] + \mathcal{O}(v)^4, \quad (38) \end{aligned}$$

and

$$\begin{aligned} \Re V(\mathbf{r} \perp \mathbf{v}, T) \approx & -\alpha_s m_D C_F \left[1 + \frac{e^{-\hat{r}}}{\hat{r}} + v^2 \left\{ \frac{3}{\hat{r}^3} - \frac{e^{-\hat{r}}}{2} \left(\frac{6}{\hat{r}^3} + \frac{6}{\hat{r}^2} + \frac{3}{\hat{r}} + 1 \right) \right. \right. \\ & - \left. \frac{\pi^2}{4} \left(\frac{1}{\hat{r}^3} - \frac{1}{24} \right) + \frac{e^{-\hat{r}} \pi^2}{4} \left(\frac{1}{\hat{r}^3} + \frac{1}{\hat{r}^2} + \frac{1}{2\hat{r}} + \frac{1}{8} \right) \right\} \Big] \\ & + \frac{2\sigma}{m_D} \left[1 + \frac{e^{-\hat{r}} - 1}{\hat{r}} + v^2 \left\{ \frac{6}{\hat{r}^3} - \frac{1}{2\hat{r}} - \frac{e^{-\hat{r}}}{2} \left(\frac{12}{\hat{r}^3} + \frac{12}{\hat{r}^2} + \frac{5}{\hat{r}} + 1 \right) \right. \right. \\ & + \left. \left. \frac{\pi^2}{4} \left(\frac{3}{\hat{r}^3} - \frac{1}{2\hat{r}} + \frac{1}{8} \right) + \frac{e^{-\hat{r}} \pi^2}{4} \left(\frac{3}{\hat{r}^3} + \frac{3}{\hat{r}^2} + \frac{1}{\hat{r}} + \frac{1}{8} \right) \right\} \right] + \mathcal{O}(v)^4. \quad (39) \end{aligned}$$

Note that zero velocity part of the potential in Eq. (38) and Eq. (39) reproduces previous isotropy potential calculation [71] and also reproduces the isotropic part of the real part of the potential in [72, 73].

B. Imaginary part of the potential

The imaginary part of the potential, $\Im V(\mathbf{r}, T, \mathbf{v})$ from Eq. (33) can be written as

$$\begin{aligned} \Im V(\mathbf{r}, T, \mathbf{v}) &= \int \frac{d^3 \mathbf{p}}{(2\pi)^{3/2}} (e^{i\mathbf{p} \cdot \mathbf{r}} - 1) V(p) \frac{p^2}{2} D_S^L(\mathbf{p}, u) \\ &= \int \frac{d^3 \mathbf{p}}{(2\pi)^{3/2}} (e^{i\mathbf{p} \cdot \mathbf{r}} - 1) \left(\sqrt{(2/\pi)} C_F \alpha_s + \frac{4\sigma}{\sqrt{2\pi} p^2} \right) \\ &\quad \times \frac{\pi m_D^2 T (1 - v^2)^{3/2} (2 + v^2 \sin^2 \theta)}{2p(1 - v^2 \sin^2 \theta)^{5/2} (p^2 + \Pi_R(\mathbf{p}, u)) (p^2 + \Pi_R^*(\mathbf{p}, u))}. \quad (40) \end{aligned}$$

We can decompose the total imaginary potential into the Coulombic and the string term as

$$\Im V(\mathbf{r}, T, \mathbf{v}) = \Im V_1(\mathbf{r}, T, \mathbf{v}) + \Im V_2(\mathbf{r}, T, \mathbf{v}). \quad (41)$$

For the first case, when the dipole aligned parallel to the direction of the relative velocity (v) between the dipole and the thermal bath, Coulombic part of the imaginary potential ($\Im V_1(r, T, u)$)

can be written as

$$\begin{aligned}
\Im V_1(\mathbf{r} \parallel \mathbf{v}, T) &= \frac{\alpha_s C_F}{2\pi^2} \int d^3\mathbf{p} (e^{i\mathbf{p}\cdot\mathbf{r}} - 1) \frac{\pi m_D^2 T (1 - v^2)^{3/2} (2 + v^2 \sin^2 \theta)}{2(1 - v^2 \sin^2 \theta)^{5/2}} \\
&\quad \times \frac{1}{p(p^2 + \Pi_R(p, u))(p^2 + \Pi_R^*(p, u))} \\
&= -2\alpha_s T C_F \int_0^{\pi/2} d\theta \sin \theta \frac{(1 - v^2)^{3/2} (2 + v^2 \sin^2 \theta)}{2(1 - v^2 \sin^2 \theta)^{5/2}} \frac{m_D^2}{\Pi_R^\parallel(\theta, v) - \Pi_R^{*\parallel}(\theta, v)} \\
&\quad + \left[\left\{ \log x^\parallel(\theta, v) + \sinh(x^\parallel(\theta, v)) \text{Shi}(x^\parallel(\theta, v)) - \cosh(x^\parallel(\theta, v)) \text{Chi}(x^\parallel(\theta, v)) \right\} \right. \\
&\quad \left. - \left\{ \log y^\parallel(\theta, v) + \sinh(y^\parallel(\theta, v)) \text{Shi}(y^\parallel(\theta, v)) - \cosh(y^\parallel(\theta, v)) \text{Chi}(y^\parallel(\theta, v)) \right\} \right], \tag{42}
\end{aligned}$$

where

$$x^\parallel = m_D r \cos \theta \sqrt{\Pi_R^\parallel(\theta, v)/m_D^2}, \tag{43}$$

$$y^\parallel = m_D r \cos \theta \sqrt{\Pi_R^{*\parallel}(\theta, v)/m_D^2}. \tag{44}$$

and $\text{Shi}(x)$ and $\text{Chi}(x)$ denotes *Mathematica* defined functions *SinhIntegral(x)* and *CoshIntegral(x)* respectively and can be expressed mathematically as

$$\text{Shi}(x) = \int_0^x \frac{\sinh t}{t} dt \quad \text{and} \quad \text{Chi}(x) = \gamma_E + \log x + \int_0^x \frac{\cosh t - 1}{t} dt. \tag{45}$$

and the string part can be written as

$$\begin{aligned}
\Im V_2(\mathbf{r} \parallel \mathbf{v}, T) &= \frac{4\sigma}{(2\pi)^2} \int d^3\mathbf{p} (e^{i\mathbf{p}\cdot\mathbf{r}} - 1) \frac{\pi m_D^2 T (1 - v^2)^{3/2} (2 + v^2 \sin^2 \theta)}{2(1 - v^2 \sin^2 \theta)^{5/2}} \\
&\quad \times \frac{1}{p^3(p^2 + \Pi_R(p, u))(p^2 + \Pi_R^*(p, u))} \\
&= 4\sigma T \int_0^{\pi/2} d\theta \sin \theta \frac{(1 - v^2)^{3/2} (2 + v^2 \sin^2 \theta)}{2(1 - v^2 \sin^2 \theta)^{5/2}} \frac{m_D^2}{\Pi_R^\parallel(\theta, v) - \Pi_R^{*\parallel}(\theta, v)} \\
&\quad \left[\frac{\gamma_E + \log x^\parallel(\theta, v) + \sinh(x^\parallel(\theta, v)) \text{Shi}(x^\parallel(\theta, v)) - \cosh(x^\parallel(\theta, v)) \text{Chi}(x^\parallel(\theta, v))}{\Pi_R^\parallel(\theta, v)} \right. \\
&\quad \left. - \frac{\gamma_E + \log y^\parallel(\theta, v) + \sinh(y^\parallel(\theta, v)) \text{Shi}(y^\parallel(\theta, v)) - \cosh(y^\parallel(\theta, v)) \text{Chi}(y^\parallel(\theta, v))}{\Pi_R^{*\parallel}(\theta, v)} \right]. \tag{46}
\end{aligned}$$

For the second case, when the dipole is aligned perpendicular to the direction of the relative velocity (v) between the dipole and the thermal bath, Coulombic part of the imaginary potential

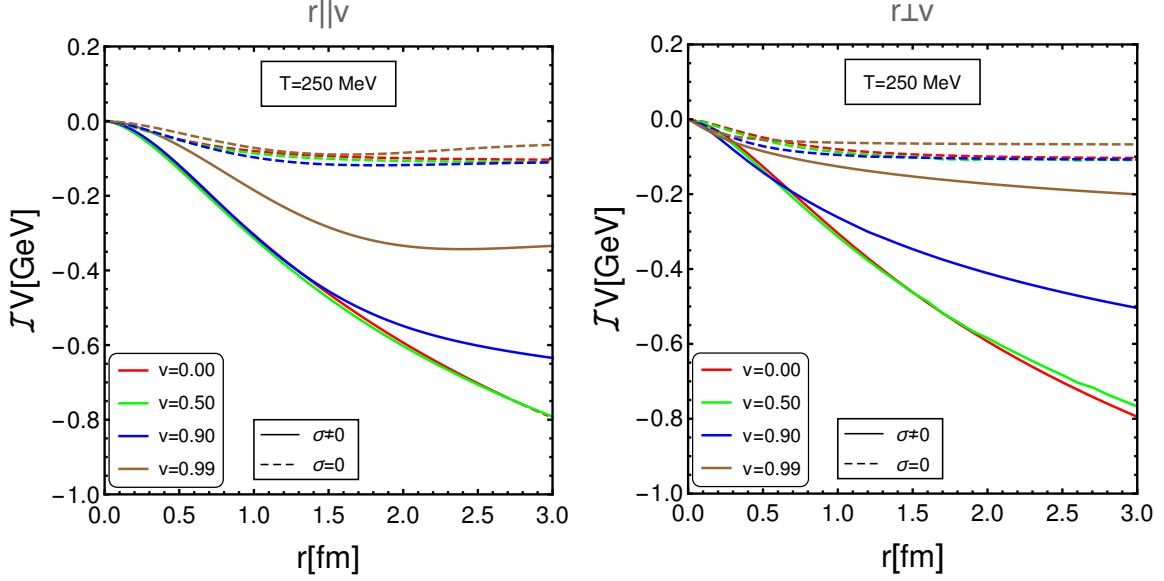


FIG. 5. Variation of imaginary part of the potential with the separation distance r between Q and \bar{Q} for various values of velocity at $T = 250$ MeV when the dipole axis is along the velocity direction (left) and perpendicular direction (right).

can be written as

$$\begin{aligned} \Im V_1(\mathbf{r} \perp \mathbf{v}, T) = & -2\alpha_s T C_F \int_0^{\pi/2} d\theta \sin \theta \int_0^{2\pi} \frac{d\phi}{2\pi} \frac{(1-v^2)^{3/2} (2+v^2-v^2 \cos^2(\phi-\beta) \sin^2 \theta)}{2(1-v^2+v^2 \sin^2 \theta \cos^2(\phi-\beta))^{5/2}} \frac{m_D^2}{\Pi_R^\perp - \Pi^{*\perp}} \\ & + \left[\left\{ \log x^\perp + \sinh(x^\perp) \text{Shi}(x^\perp) - \cosh(x^\perp) \text{Chi}(x^\perp) \right\} \right. \\ & \left. - \left\{ \log y^\perp + \sinh(y^\perp) \text{Shi}(y^\perp) - \cosh(y^\perp) \text{Chi}(y^\perp) \right\} \right], \end{aligned} \quad (47)$$

where

$$x^\perp = m_D r \cos \theta \sqrt{\Pi_R^\perp(\theta, \phi, \beta, v)/m_D^2}, \quad (48)$$

$$y^\perp = m_D r \cos \theta \sqrt{\Pi_R^{*\perp}(\theta, \phi, \beta, v)/m_D^2}. \quad (49)$$

Similarly, the string part can be written as

$$\begin{aligned} \Im V_2(\mathbf{r} \perp \mathbf{v}, T) = & \frac{4\sigma T}{m_D^2} \int_0^{\pi/2} d\theta \sin \theta \int_0^{2\pi} \frac{d\phi}{2\pi} \frac{(1-v^2)^{3/2} (2+v^2-v^2 \cos^2(\phi-\beta) \sin^2 \theta)}{2(1-v^2+v^2 \sin^2 \theta \cos^2(\phi-\beta))^{5/2}} \frac{m_D^2}{\Pi_R^\perp - \Pi^{*\perp}} \\ & \times \left[\frac{m_D^2}{\Pi_R^\perp} \left\{ \gamma_E + \log x^\perp + \sinh(x^\perp) \text{Shi}(x^\perp) - \cosh(x^\perp) \text{Chi}(x^\perp) \right\} \right. \\ & \left. - \frac{m_D^2}{\Pi_R^{*\perp}} \left\{ \gamma_E + \log y^\perp + \sinh(y^\perp) \text{Shi}(y^\perp) - \cosh(y^\perp) \text{Chi}(y^\perp) \right\} \right]. \end{aligned} \quad (50)$$

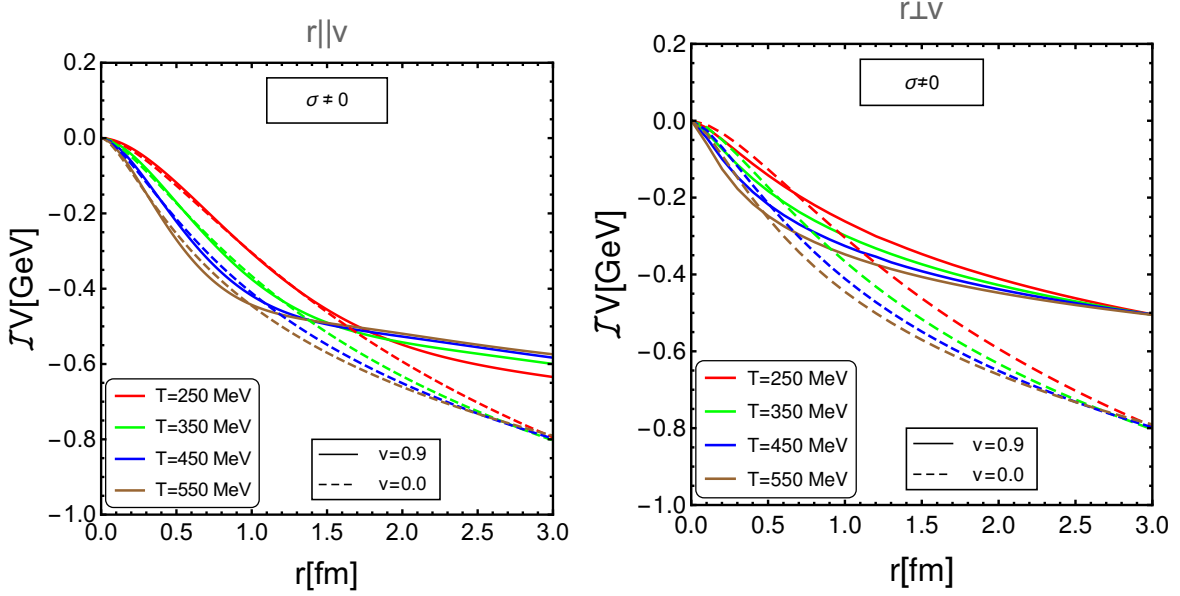


FIG. 6. Variation of the imaginary part of the potential with the separation distance r between Q and \bar{Q} for various values of temperature when the dipole axis is along the velocity direction (left) and perpendicular direction (right).

From the Fig. 5, we find that the imaginary part of the potential decreases in magnitude at ultra-relativistic velocities and approaches zero. Thus it contributes less to the decay width for both the cases at large velocities. The imaginary part increases (in magnitude) with the inclusion of the string term ($\sigma \neq 0$) as compared to the Coulombic term alone for both the cases. The decrease in magnitude at large velocities is more for the perpendicular case as compared to the parallel case. The imaginary part vanishes at the origin for any value of v for both the parallel and perpendicular case. Fig. 6 shows the variation of the imaginary part of the potential with the separation distance r for various values of temperature with solid lines for $v = 0.9$ and dotted lines for $v = 0$. From the figure we find that imaginary part of the potential increases in magnitude with increase in temperature and hence, contributes more to the decay width. The increase in magnitude is more at short distances as compared to large distances.

Similar to the real part of the potential in Eq. (37), the imaginary part of the potential at any orientation can be written as

$$\Im V(\mathbf{r}, T, \mathbf{v}) = \frac{1}{2} \Im V(\mathbf{r} \parallel \mathbf{v}, T) (1 + \cos 2\theta_{vr}) + \frac{1}{2} \Im V(\mathbf{r} \perp \mathbf{v}, T) (1 - \cos 2\theta_{vr}). \quad (51)$$

Similar to real part of the potential, it is possible to calculate angular integration analytically when the relative velocity is small. For small and moderate velocity, imaginary part of the potential

in the parallel alignment case can be written as

$$\begin{aligned}
\Im V(\mathbf{r} \parallel \mathbf{v}, T) \approx & -\alpha_s T C_F \left[1 + \frac{\sinh \hat{r} (\hat{r} \text{Shi } \hat{r} + \text{Chi } \hat{r}) - \cosh \hat{r} (\text{Shi } \hat{r} + \hat{r} \text{Chi } \hat{r})}{\hat{r}} - \frac{(35\pi^2 - 432) (\hat{r}^2 + 18)}{576\hat{r}^2} v^2 \right. \\
& + \frac{v^2}{192\hat{r}^3} \left\{ \left(\text{Chi}(\hat{r}) \sinh(\hat{r}) - \text{Shi}(\hat{r}) \cosh(\hat{r}) \right) \left(8 (\pi^2 - 12) \hat{r}^4 + 3 (35\pi^2 - 432) (\hat{r}^2 + 2) \right) \right. \\
& \left. \left. - \left(\text{Chi}(\hat{r}) \cosh(\hat{r}) - \text{Shi}(\hat{r}) \sinh(\hat{r}) \right) \left(\pi^2 \hat{r}^4 + (35\pi^2 - 432) (\hat{r}^2 + 6) \right) \hat{r} \right\} \right] \\
& - \frac{\sigma T}{m_D^2} \left[(3 - 2\gamma_E - 2 \log \hat{r}) + \frac{\sinh \hat{r} (\hat{r} \text{Shi } \hat{r} + 3 \text{Chi } \hat{r}) - \cosh \hat{r} (3 \text{Shi } \hat{r} + \hat{r} \text{Chi } \hat{r})}{\hat{r}} \right. \\
& + v^2 \left\{ \frac{\hat{r}^2 (16 (\pi^2 - 6) (\log(\hat{r}) + \gamma_E) - 35\pi^2 + 112) + 90 (80 - 7\pi^2)}{192\hat{r}^2} \right. \\
& + \frac{(48 (2\hat{r}^4 + 69\hat{r}^2 + 150) - 7\pi^2 (2\hat{r}^4 + 45\hat{r}^2 + 90)) (\text{Chi}(\hat{r}) \sinh(\hat{r}) - \text{Shi}(\hat{r}) \cosh(\hat{r}))}{192\hat{r}^3} \\
& \left. \left. + \frac{(\pi^2 (\hat{r}^4 + 89\hat{r}^2 + 630) - 48 (17\hat{r}^2 + 150)) \hat{r} (\text{Chi}(\hat{r}) \cosh(\hat{r}) - \text{Shi}(\hat{r}) \sinh(\hat{r}))}{192\hat{r}^3} \right\} \right] + \mathcal{O}(v)^4. \tag{52}
\end{aligned}$$

In addition to the parallel case at small velocity, imaginary part of the potential in the perpendicular alignment case can be written as

$$\begin{aligned}
\Im V(\mathbf{r} \perp \mathbf{v}, T) \approx & -\alpha_s T C_F \left[1 + \frac{\sinh \hat{r} (\hat{r} \text{Shi } \hat{r} + \text{Chi } \hat{r}) - \cosh \hat{r} (\text{Shi } \hat{r} + \hat{r} \text{Chi } \hat{r})}{\hat{r}} - \left\{ \frac{27}{4\hat{r}^2} + \frac{5 (\hat{r}^2 - 18)}{576\hat{r}^2} \right\} v^2 \right. \\
& + \frac{v^2}{192\hat{r}^3} \left\{ \left(\text{Chi}(\hat{r}) \cosh(\hat{r}) - \text{Shi}(\hat{r}) \sinh(\hat{r}) \right) \left(144 (\hat{r}^2 + 9) - 5\pi^2 (2\hat{r}^2 + 21) \right) \hat{r} \right. \\
& \left. \left. - \left(\text{Chi}(\hat{r}) \sinh(\hat{r}) - \text{Shi}(\hat{r}) \cosh(\hat{r}) \right) \left(48 (\hat{r}^2 + 3) (\hat{r}^2 + 9) - \pi^2 (\hat{r}^4 + 45\hat{r}^2 + 105) \right) \hat{r} \right\} \right] \\
& - \frac{\sigma T}{m_D^2} \left[(3 - 2\gamma_E - 2 \log \hat{r}) + \frac{\sinh \hat{r} (\hat{r} \text{Shi } \hat{r} + 3 \text{Chi } \hat{r}) - \cosh \hat{r} (3 \text{Shi } \hat{r} + \hat{r} \text{Chi } \hat{r})}{\hat{r}} \right. \\
& + v^2 \left\{ \frac{\hat{r}^2 (16 (\pi^2 - 6) (\log(\hat{r}) + \gamma) - 35\pi^2 + 160) + 45 (7\pi^2 - 80)}{192\hat{r}^2} \right. \\
& - \frac{(48 (\hat{r}^4 + 30\hat{r}^2 + 75) - \pi^2 (\hat{r}^4 + 105\hat{r}^2 + 315)) (\text{Chi}(\hat{r}) \sinh(\hat{r}) - \text{Shi}(\hat{r}) \cosh(\hat{r}))}{192\hat{r}^3} \\
& \left. \left. + \frac{(48 (7\hat{r}^2 + 75) - \pi^2 (16\hat{r}^2 + 315)) \hat{r} (\text{Chi}(\hat{r}) \cosh(\hat{r}) - \text{Shi}(\hat{r}) \sinh(\hat{r}))}{192\hat{r}^3} \right\} \right] + \mathcal{O}(v)^4. \tag{53}
\end{aligned}$$

Furthermore, Eqs. (52) and (53) can be expanded and can be written in compact form when

the $Q\bar{Q}$ separation is small as

$$\begin{aligned} \Im V(\mathbf{r} \parallel \mathbf{v}, T) \stackrel{\hat{r} \ll 1}{\approx} -\alpha_s T C_F \left[\frac{1}{9} (4 - 3\gamma_E - 3 \log \hat{r}) \hat{r}^2 + v^2 \left(\frac{2}{25} + \frac{\gamma_E}{10} - \frac{\pi^2}{240} - \frac{\log \hat{r}}{10} \right) \hat{r}^2 + \mathcal{O}(\hat{r})^4 \right] \\ - \frac{2\sigma T}{m_D^2} \left[\frac{\hat{r}^2}{6} + \frac{-107 + 60\gamma_E + 60 \log \hat{r}}{3600} \hat{r}^4 \right. \\ \left. + \frac{v^2}{120} \left\{ (10 - \pi^2) \hat{r}^2 + \left(\frac{887}{980} - \frac{9\gamma_E + \log \hat{r}}{7} + \frac{5\pi^2}{168} \right) \hat{r}^4 \right\} + \mathcal{O}(\hat{r})^6 \right] + \mathcal{O}(v)^4 \end{aligned} \quad (54)$$

and

$$\begin{aligned} \Im V(\mathbf{r} \perp \mathbf{v}, T) \stackrel{\hat{r} \ll 1}{\approx} -\alpha T C_F \left[\frac{1}{9} (4 - 3\gamma_E - 3 \log \hat{r}) \hat{r}^2 + v^2 \left(\frac{22}{75} - \frac{3\gamma_E}{10} - \frac{\pi^2}{720} - \frac{3 \log \hat{r}}{10} \right) \hat{r}^2 + \mathcal{O}(\hat{r})^4 \right] \\ - \frac{2\sigma T}{m_D^2} \left[\frac{\hat{r}^2}{6} + \frac{-107 + 60\gamma_E + 60 \log \hat{r}}{3600} \hat{r}^4 \right. \\ \left. + \frac{v^2}{360} \left\{ (30 - \pi^2) \hat{r}^2 - \left(\frac{1839}{196} - \frac{45(\gamma_E + \log \hat{r})}{7} - \frac{\pi^2}{56} \right) \hat{r}^4 \right\} + \mathcal{O}(\hat{r})^6 \right] + \mathcal{O}(v)^4. \end{aligned} \quad (55)$$

Note that $v = 0$ part of the approximate imaginary part potential given in Eqs. (54) and (55) matches with the isotropic part of the previously calculated imaginary potential in anisotropic medium [73].

VI. THERMAL WIDTH

The imaginary part of the potential is a perturbation to the vacuum potential and thus provides an estimate for the thermal width ($\Gamma_{Q\bar{Q}}$) for a resonance state and can be calculated, in a first-order perturbation from the imaginary part of the potential as

$$\Gamma_{Q\bar{Q}} = -\langle \psi | \Im V_{Q\bar{Q}}(\mathbf{r}, T, \mathbf{v}) | \psi \rangle, \quad (56)$$

where ψ is the Coulombic wave function for the ground state and is given by

$$\psi(\mathbf{r}) = \frac{1}{\sqrt{\pi a_0^3}} e^{-r/a_0}, \quad (57)$$

where $a_0 = 2/(C_F m_Q \alpha_s)$ is the Bohr radius of the $Q\bar{Q}$ system. Even though the imaginary potential is not purely Coulombic but the leading contribution to the potential for the deeply bound $Q\bar{Q}$ states in a plasma is Coulombic, thus justifying the use of Coulomb-like wave functions to determine the width.

Using Eqs. (56) and (57), the decay width of quarkonium in the moving thermal medium can be written as

$$\begin{aligned} \Gamma &= -\frac{1}{\pi a_0^3} \int d^3 \mathbf{r} e^{-2r/a_0} \Im V_{Q\bar{Q}}(\mathbf{r}, T, \mathbf{v}) \\ &= -\frac{1}{\pi a_0^3} \int_0^\infty d^3 \mathbf{r} e^{-2r/a_0} \int \frac{d^3 \mathbf{p}}{(2\pi)^{3/2}} (e^{i\mathbf{p} \cdot \mathbf{r}} - 1) \left(\sqrt{2/\pi} C_F \alpha_s + \frac{4\sigma}{\sqrt{2\pi} p^2} \right) \\ &\quad \times \frac{\pi m_D^2 T (1 - v^2)^{3/2} (2 + v^2 \sin^2 \theta)}{2p (1 - v^2 \sin^2 \theta)^{5/2} (p^2 + \Pi_R(\mathbf{p}, u)) (p^2 + \Pi_R^*(\mathbf{p}, u))} \\ &= \Gamma_1 + \Gamma_2, \end{aligned} \quad (58)$$

where Γ_1 and Γ_2 are the thermal widths for the Coulombic and the string parts respectively. Width (Γ_1) for the Coulombic part:

$$\Gamma_1 = -\frac{\alpha_s m_D^2 T C_F}{2\pi^2 a_0^3} \int d^3 \mathbf{r} e^{-2r/a_0} \int d^3 \mathbf{p} (e^{i\mathbf{p}\cdot\mathbf{r}} - 1) \frac{(1-v^2)^{3/2} (2+v^2 \sin^2 \theta)}{2(1-v^2 \sin^2 \theta)^{5/2}} \times \frac{1}{p(p^2 + \Pi_R(\mathbf{p}, u))(p^2 + \Pi_R^*(\mathbf{p}, u))}. \quad (59)$$

We can analytically integrate over $Q\bar{Q}$ separation distance r . After doing the r integration analytically, Eq. (59) reduces to

$$\Gamma_1 = \alpha_s m_D^2 T C_F \int_{-1}^1 d(\cos \theta) f(v, \theta) \int_0^\infty \frac{p dp}{(p^2 + \Pi_R(\theta, v))(p^2 + \Pi_R^*(\theta, v))} \left(1 - \frac{1}{\left(1 + \frac{p^2 a_0^2}{4}\right)^2} \right), \quad (60)$$

where

$$f(v, \theta) = \frac{(1-v^2)^{3/2} (2+v^2 \sin^2 \theta)}{2(1-v^2 \sin^2 \theta)^{5/2}}. \quad (61)$$

and

$$\Pi_R(\theta, v) = \frac{m_D^2}{2} \left[\frac{2 - 2v^2 - v^4 \cos^2 \theta \sin^2 \theta}{(1 - v^2 \sin^2 \theta)^2} - \frac{(2 + v^2 \sin^2 \theta)(1 - v^2)v \cos \theta}{2(1 - v^2 \sin^2 \theta)^{5/2}} \times \log \left(\frac{v \cos \theta + \sqrt{1 - v^2 \sin^2 \theta}}{v \cos \theta - \sqrt{1 - v^2 \sin^2 \theta}} \right) \right]. \quad (62)$$

We can again perform the momentum integration analytically. After performing the integration over momentum p , Eq. (60) becomes

$$\Gamma_1 = -\alpha_s m_D^2 T C_F \int_{-1}^1 d(\cos \theta) f(v, \theta) \left[\frac{2a_0^2}{(a_0^2 \Pi_R(\theta, v) - 4)(a_0^2 \Pi_R^*(\theta, v) - 4)} - \frac{1}{2(\Pi_R(\theta, v) - \Pi_R^*(\theta, v))} \times \left\{ \left(1 - \frac{16}{(a_0^2 \Pi_R(\theta, v) - 4)^2} \right) \log \Pi_R(\theta, v) - \left(1 - \frac{16}{(a_0^2 \Pi_R^*(\theta, v) - 4)^2} \right) \log \Pi_R^*(\theta, v) \right\} + \frac{16a_0^2 (8 - a_0^2 \Pi_R(\theta, v) - a_0^2 \Pi_R^*(\theta, v))}{(a_0^2 \Pi_R(\theta, v) - 4)^2 (a_0^2 \Pi_R^*(\theta, v) - 4)^2} \log \left(\frac{a_0}{2} \right) \right]. \quad (63)$$

At $v = 0$, the above equation reduces to

$$\Gamma_1(v = 0) = \frac{\alpha_s m_D^2 a_0^2 T C_F}{(a_0^2 m_D^2 - 4)} \left[1 - \frac{8}{(a_0^2 m_D^2 - 4)} + \frac{64}{(a_0^2 m_D^2 - 4)^2} \log \frac{m_D a_0}{2} \right]. \quad (64)$$

Thermal width (Γ_2) for the string (non-perturbative) part is

$$\begin{aligned}
\Gamma_2 &= -\frac{4\sigma m_D^2 T}{(2\pi)^2 a_0^3} \int d^3\mathbf{r} e^{-2r/a_0} \int d^3\mathbf{p} (e^{i\mathbf{p}\cdot\mathbf{r}} - 1) \frac{(1-v^2)^{3/2}(2+v^2\sin^2\theta)}{2(1-v^2\sin^2\theta)^{5/2}} \\
&\quad \times \frac{1}{p^3 (p^2 + \Pi_R(\mathbf{p}, u)) (p^2 + \Pi_R^*(\mathbf{p}, u))} \\
&= 2\sigma m_D^2 T \int_{-1}^1 d(\cos\theta) f(v, \theta) \int_0^\infty \frac{dp}{p(p^2 + \Pi_R(\theta, v)) (p^2 + \Pi_R^*(\theta, v))} \\
&\quad \times \left(1 - \frac{1}{\left(1 + \frac{p^2 a_0^2}{4}\right)^2} \right). \tag{65}
\end{aligned}$$

After performing the integration over \mathbf{p} , Eq. 65 becomes

$$\begin{aligned}
\Gamma_2 &= \sigma m_D^2 a_0^2 T \int_{-1}^1 d(\cos\theta) f(v, \theta) \left[\frac{a_0^2}{(a_0^2 \Pi_R(\theta, v) - 4) (a_0^2 \Pi_R^*(\theta, v) - 4)} \right. \\
&\quad + \frac{2a_0^2 (a_0^4 \Pi_R(\theta, v) \Pi_R^*(\theta, v) - 8a_0^2 (\Pi_R(\theta, v) + \Pi_R^*(\theta, v)) + 48)}{(a_0^2 \Pi_R(\theta, v) - 4)^2 (a_0^2 \Pi_R^*(\theta, v) - 4)^2} \log \frac{a_0}{2} - \frac{1}{\Pi_R(\theta, v) - \Pi_R^*(\theta, v)} \\
&\quad \times \left. \left\{ \frac{(a_0^2 \Pi_R - 8)}{(a_0^2 \Pi_R(\theta, v) - 4)^2} \log \Pi_R(\theta, v) - \frac{(a_0^2 \Pi_R^*(\theta, v) - 8)}{(a_0^2 \Pi_R^*(\theta, v) - 4)^2} \log \Pi_R^*(\theta, v) \right\} \right]. \tag{66}
\end{aligned}$$

At $v = 0$, the above equation reduces to

$$\Gamma_2(v=0) = \frac{4\sigma a_0^2 T}{(a_0^2 m_D^2 - 4)^2} \left[4 + \frac{a_0^2 m_D^2 (a_0^2 m_D^2 - 12)}{(a_0^2 m_D^2 - 4)} \log \frac{m_D a_0}{2} \right]. \tag{67}$$

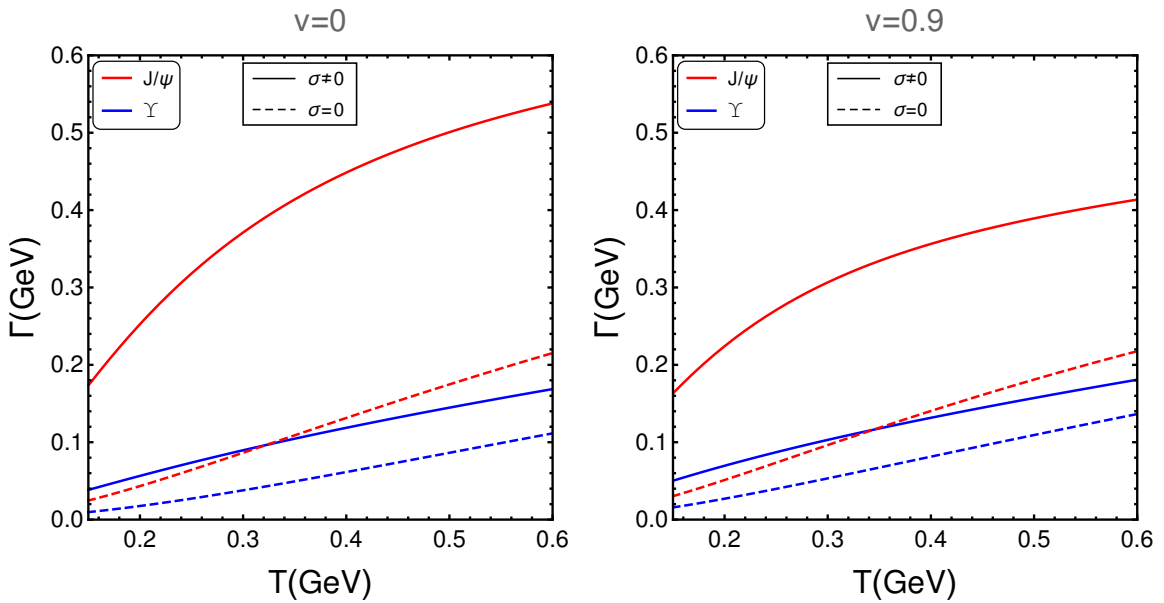


FIG. 7. Variation of decay width with temperature T for J/ψ and Υ for $v = 0$ (left) and $v = 0.9$ (right).

Total decay width after substituting Eqs. (63) and (66) into Eq. (58)

$$\begin{aligned}
\Gamma = & -m_D^2 T \int_{-1}^1 d(\cos \theta) f(v, \theta) \left[C_F \alpha_s \left\{ \frac{2a_0^2}{(a_0^2 \Pi_R(\theta, v) - 4)(a_0^2 \Pi_R^*(\theta, v) - 4)} - \frac{1}{2(\Pi_R(\theta, v) - \Pi_R^*(\theta, v))} \right. \right. \\
& \times \left(\left(1 - \frac{16}{(a_0^2 \Pi_R(\theta, v) - 4)^2} \right) \log \Pi_R(\theta, v) - \left(1 - \frac{16}{(a_0^2 \Pi_R^*(\theta, v) - 4)^2} \right) \log \Pi_R^*(\theta, v) \right) \\
& + \frac{16a_0^2 (8 - a_0^2 \Pi_R(\theta, v) - a_0^2 \Pi_R^*(\theta, v))}{(a_0^2 \Pi_R(\theta, v) - 4)^2 (a_0^2 \Pi_R^*(\theta, v) - 4)^2} \log \left(\frac{a_0}{2} \right) \Big\} - \sigma a_0^2 \left\{ \frac{a_0^2}{(a_0^2 \Pi_R(\theta, v) - 4)(a_0^2 \Pi_R^*(\theta, v) - 4)} \right. \\
& - \frac{1}{\Pi_R(\theta, v) - \Pi_R^*(\theta, v)} \left(\frac{(a_0^2 \Pi_R - 8)}{(a_0^2 \Pi_R(\theta, v) - 4)^2} \log \Pi_R(\theta, v) - \frac{(a_0^2 \Pi_R^*(\theta, v) - 8)}{(a_0^2 \Pi_R^*(\theta, v) - 4)^2} \log \Pi_R^*(\theta, v) \right) \\
& \left. \left. + \frac{2a_0^2 (a_0^4 \Pi_R(\theta, v) \Pi_R^*(\theta, v) - 8a_0^2 (\Pi_R(\theta, v) + \Pi_R^*(\theta, v)) + 48)}{(a_0^2 \Pi_R(\theta, v) - 4)^2 (a_0^2 \Pi_R^*(\theta, v) - 4)^2} \log \frac{a_0}{2} \right\} \right]. \quad (68)
\end{aligned}$$

Note that we compute the momentum integration analytically in all the cases *viz.* real part of the potential, imaginary part of the potential and thermal width calculations for both the Coulombic and the string terms. We also compute the trivial azimuthal integration analytically in some cases. We only calculate the non-trivial angular integration numerically. But in Refs. [49, 50], the authors have done both the angular and the momentum integration numerically for the Coulombic term (except the trivial azimuthal integration.)

We show numerically the variation of total decay width (Eq. (68)) with temperature for the ground state of charmonium and bottomonium in Fig. 7. We take charmonium and bottomonium masses as $m_c = 1.275$ GeV and $m_b = 4.66$ GeV respectively from [84]. We find that the thermal width increases with increase of the temperature and the increase in width with inclusion of the string term is more as compared to the earlier result with the Coulombic term alone [62]. The increase in decay width is less at ultra-relativistic velocities ($v = 0.9$) as compared to the zero velocity case ($v = 0$). Width for bottomonium ground state (Υ) is much smaller than the charmonium ground state (J/ψ) because the bottomonium states are bound tighter than the charmonium states.

Alternatively, we can say that decay width decreases with increase in quark masses and dissociation begins at higher temperature. From the Fig. 8, we find that width increases with increase in temperature and decreases at ultra-relativistic velocities.

A. Approximate decay width

We can obtain the approximate solution of Eq. (60) valid at moderate velocities which fulfill the relation $1/a_0 \gg m_D$, so that the technique of threshold expansion [85] can be used to work out the integral, thus we obtain

$$\begin{aligned}
\Gamma_1 \approx & \alpha_s m_D^2 T C_F \int_{-1}^1 d(\cos \theta) f(v, \theta) \left[\log \left(\frac{2}{m_D a_0} \right) - \frac{1}{4} \right. \\
& \left. - \frac{1}{2(\Pi_R(\theta, v) - \Pi_R^*(\theta, v))} \left(\Pi_R(\theta, v) \log \frac{\Pi_R(\theta, v)}{m_D^2} - \Pi_R^*(\theta, v) \log \frac{\Pi_R^*(\theta, v)}{m_D^2} \right) + \mathcal{O}(m_D^2 a_0^2) \right]. \quad (69)
\end{aligned}$$

Eq. (69) can be further simplified by taking into account that the $\log(\frac{2}{m_D a_0})$ is logarithmically

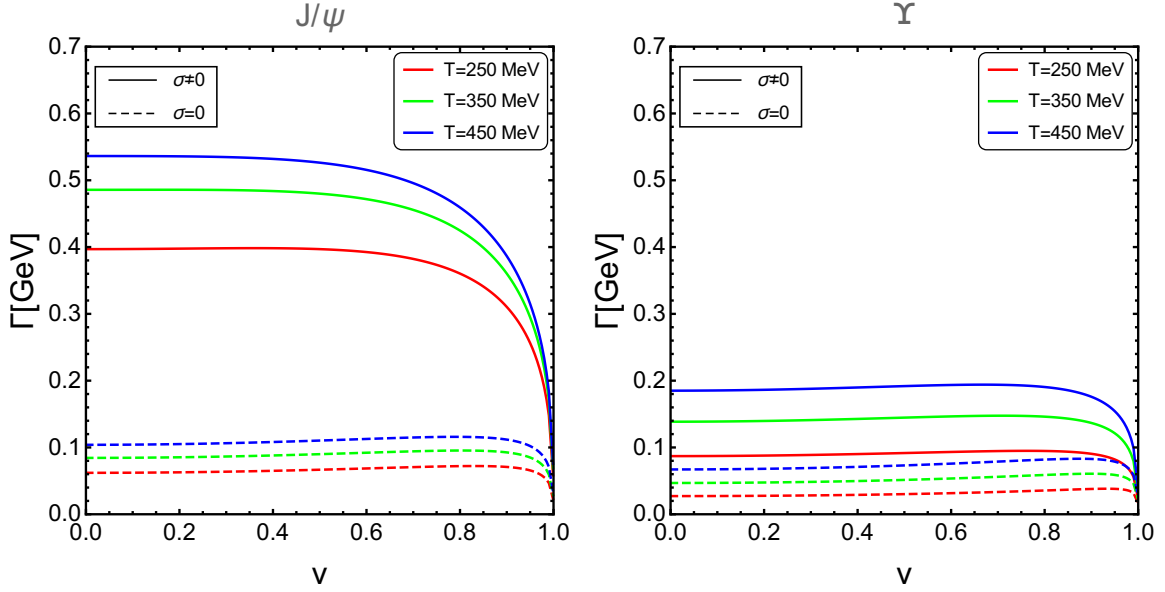


FIG. 8. Variation of decay width for $J/\psi(1S)$ (left) and $\Upsilon(1S)$ (right) states with velocity v for different values of temperature T .

bigger than the rest of the terms in the parenthesis.

$$\Gamma_1 \approx \frac{\alpha_s m_D^2 a_0^2 T C_F}{\sqrt{1-v^2}} \log \left(\frac{2}{m_D a_0} \right). \quad (70)$$

Similarly, for the string term, decay width at moderate velocities which fulfill the relation $1/a_0 \gg m_D$ can be approximated as

$$\begin{aligned} \Gamma_2 \approx & \frac{\sigma T a_0^2 m_D^2}{\sqrt{1-v^2}} \left[-\frac{3}{4} a_0^2 \log \left(\frac{2}{m_D a_0} \right) + \frac{\log \Pi_R(\theta, v) - \log \Pi_R^*(\theta, v)}{\Pi_R(\theta, v) - \Pi_R^*(\theta, v)} \right. \\ & \left. + \frac{3a_0^2}{8 (\Pi_R(\theta, v) - \Pi_R^*(\theta, v))} \left(\Pi_R(\theta, v) \log \frac{\Pi_R(\theta, v)}{m_D^2} - \Pi_R^*(\theta, v) \log \frac{\Pi_R^*(\theta, v)}{m_D^2} \right) + \mathcal{O}(m_D^2 a_0^2) \right]. \end{aligned} \quad (71)$$

Eq. (71) can be further simplified by taking into account that the $\log(\frac{2}{m_D a_0})$ is logarithmically bigger than the rest of the terms in the parenthesis, therefore after neglecting the other terms we get

$$\Gamma_2 \approx \frac{-3\sigma T a_0^4 m_D^2}{4\sqrt{(1-v^2)}} \log \left(\frac{2}{m_D a_0} \right), \quad (72)$$

and the total approximated decay width becomes

$$\Gamma \approx \frac{4m_D^2 T}{\sqrt{1-v^2}} \left(\frac{\alpha_s}{C_F \alpha_s^2 m_Q^2} - \frac{3\sigma}{C_F^4 \alpha_s^4 m_Q^4} \right) \log \left(\frac{\alpha_s C_F m_Q}{m_D} \right). \quad (73)$$

Fig. 9 shows the variation of the ratio of the total width ($\Gamma(v)/\Gamma(0)$) for $J/\psi(1S)$ and $\Upsilon(1S)$ states, for three different temperatures, for $0 \leq v \lesssim 1$ with the string term ($\sigma \neq 0$) and without the string term ($\sigma = 0$). The ratio of the width decreases for larger values of v and becomes temperature dependent. This is obvious as for $v \rightarrow 1$, Eqs. (69) and (71) do not hold and further

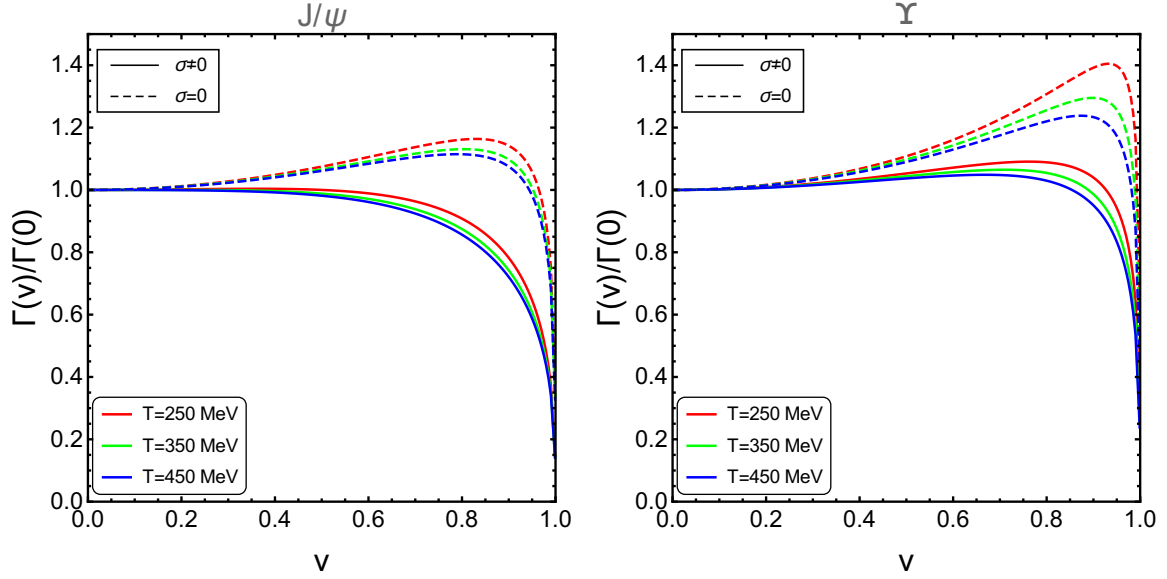


FIG. 9. Variation of the scaled decay width ($\Gamma(v)/\Gamma(0)$) for $J/\psi(1S)$ (left) and $\Upsilon(1S)$ (right) states with velocity v for different values of temperature T .

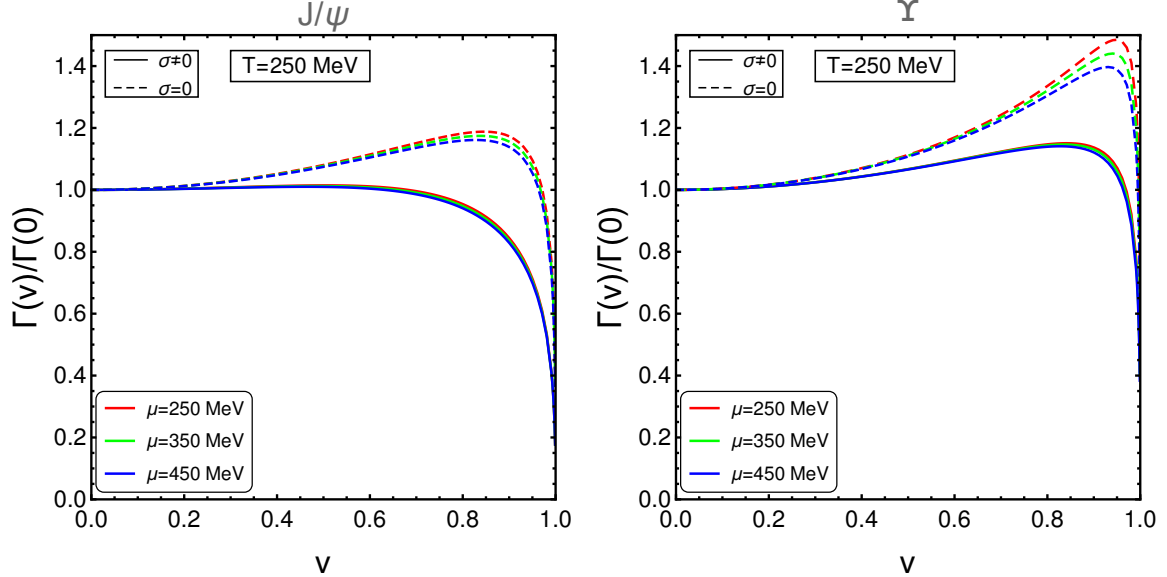


FIG. 10. Variation of the scaled decay width ($\Gamma(v)/\Gamma(0)$) for $J/\psi(1S)$ (left) and $\Upsilon(1S)$ (right) states with velocity v for different values of chemical potential μ .

scale must be considered ($T_+ \gg T \gg T_-$). The decrease in width ratio at large velocities is more with the string term as compared to the ratio without the the string term [50] and decrease is more with increase in temperature. The reason for the decrease in the decay width is probably related to the fact that a moving bound state feels a plasma with a non-isotropic effective temperature (T_{eff}) which we have introduced in section II.

Fig. 10 shows the variation of the ratio of the width ($\Gamma(v)/\Gamma(0)$) for $J/\psi(1S)$ and $\Upsilon(1S)$ states, for three different values of chemical potential, for $0 \leq v \lesssim 1$ with the string term ($\sigma \neq 0$) and

without the string term ($\sigma = 0$). The ratio of the width decreases for larger values of v and becomes very less μ dependent. We can say that width ratio has very less μ dependence.

VII. CONCLUSIONS AND OUTLOOK

In conclusion, we have studied how the real and the imaginary parts of the heavy quark-antiquark potential are modified in the presence of non-perturbative string term when there is relative motion between dipole and the thermal medium. We have modified the full Cornell potential through the dielectric function in real-time formalism using the hard thermal loop (HTL) approximation. We have reproduced the previous results for the medium at rest and extended them for non-vanishing velocities of the thermal medium. We found that the real part of potential increases with increase in velocity at short distances and becomes less screened but it decreases with the increase in velocity at large distances and becomes more screened when the $Q\bar{Q}$ pairs aligned along the motion of the medium (parallel case). On the other hand, potential decreases with increase in velocity for the perpendicular case which results in more screening of the potential. Since the $Q\bar{Q}$ potential is effectively more screened in the moving plasma, it results in earlier dissociation of quarkonium states in a moving medium. Inclusion of the string term makes the potential less screened as compared to the Coulombic term alone for both the cases. Combining all these effects we expect a stronger binding of a $Q\bar{Q}$ pair in moving medium in the presence of the string term as compared to the Coulombic term alone in the moving medium. We have also shown how the real part of the potential varies at finite μ and found a weak dependence on μ upto chemical potential as large as $\mu = 550$ MeV. We have observed an oscillatory behavior of the real part of potential at large velocities rather than exponential damping at short distances. This oscillatory behavior increases with the inclusion of the string term which leads to the stabilization of the bound state. Thus the quarkonium dissociation temperature increases with the inclusion of the string term.

The behavior of imaginary part of the potential is similar to the one determined for the static medium, but decreases (in magnitude) with increase in velocity and increases (in magnitude) with the inclusion of the string term. As a result, width of the quarkonium states get narrower at higher relative velocities and get more broadened in the presence of the string term which plays an important role in the dissociation mechanism. The reason for the decrease in the decay width in moving medium is probably related to the fact that bound states in a moving medium feel a plasma with non-isotropic effective temperature. Thus it is not obvious that width of the state in moving medium should increase or modified at all when there is relative velocity between the $Q\bar{Q}$ pair and thermal medium. However, effective temperature is almost everywhere less than T at ultra-relativistic case due to which width decreases at $v \sim 1$ and tends to stabilize the system. In this case decay width is dominated by the Landau damping. All these effects lead to the modification of the quarkonium suppression. The decay width for the bottomonium ground state is much smaller than the charmonium ground state because bottomonium state are tighter than the charmonium state and dissociation begins at high temperature. We have also extended our calculation at finite μ and found a very weak dependence of decay width on μ . In future, we would like to solve the Schrödinger equation with both the real and imaginary parts of the potential to calculate the dissociation temperature of quarkonium states by using both the Debye screening and Landau damping mechanism. It would be interesting to see the dependence of velocity on the binding energy and dissociation temperature of the heavy quarkonium states.

VIII. ACKNOWLEDGEMENT

We thank M. A. Escobedo and B. K. Patra for useful discussions. We also thank S. Chakraborty and A. Bandyopadhyay for the useful comments. NH was supported by a Postdoctoral Research Fellowship from the Alexander von Humboldt Foundation. LT sincerely acknowledges PRL, India for the Institute postdoctoral fellowship.

-
- [1] T. Matsui and H. Satz, Phys. Lett. B **178**, 416 (1986).
 - [2] F. Karsch, M. T. Mehr and H. Satz, Z. Phys. C **37**, 617 (1988).
 - [3] R. Rapp, D. Blaschke and P. Crochet, Prog. Part. Nucl. Phys. **65**, 209 (2010) [arXiv:0807.2470 [hep-ph]].
 - [4] A. Mocsy, P. Petreczky and M. Strickland, Int. J. Mod. Phys. A **28**, 1340012 (2013) [arXiv:1302.2180 [hep-ph]].
 - [5] A. Mocsy and P. Petreczky, Phys. Rev. D **77**, 014501 (2008) [arXiv:0705.2559 [hep-ph]].
 - [6] A. Mocsy and P. Petreczky, Phys. Rev. Lett. **99**, 211602 (2007) [arXiv:0706.2183 [hep-ph]].
 - [7] C. Y. Wong, Phys. Rev. C **72**, 034906 (2005) [hep-ph/0408020].
 - [8] A. Mocsy and P. Petreczky, Phys. Rev. D **73**, 074007 (2006) [hep-ph/0512156].
 - [9] W. M. Alberico, A. Beraudo, A. De Pace and A. Molinari, Phys. Rev. D **77**, 017502 (2008) [arXiv:0706.2846 [hep-ph]].
 - [10] F. Karsch, M. G. Mustafa and M. H. Thoma, Phys. Lett. B **497**, 249 (2001) [hep-ph/0007093].
 - [11] D. Cabrera and R. Rapp, Phys. Rev. D **76**, 114506 (2007) [hep-ph/0611134].
 - [12] A. Mocsy and P. Petreczky, Eur. Phys. J. C **43**, 77 (2005) [hep-ph/0411262].
 - [13] T. Umeda, K. Nomura and H. Matsufuru, Eur. Phys. J. C **39S1**, 9 (2005) [hep-lat/0211003].
 - [14] M. Asakawa and T. Hatsuda, Phys. Rev. Lett. **92**, 012001 (2004) [hep-lat/0308034].
 - [15] S. Datta, F. Karsch, P. Petreczky and I. Wetzorke, Phys. Rev. D **69**, 094507 (2004) [hep-lat/0312037].
 - [16] A. Jakovac, P. Petreczky, K. Petrov and A. Velytsky, Phys. Rev. D **75**, 014506 (2007) [hep-lat/0611017].
 - [17] G. Aarts, C. Allton, M. B. Oktay, M. Peardon and J. I. Skullerud, Phys. Rev. D **76**, 094513 (2007) [arXiv:0705.2198 [hep-lat]].
 - [18] H. T. Ding, A. Francis, O. Kaczmarek, F. Karsch, H. Satz and W. Soeldner, Phys. Rev. D **86**, 014509 (2012) [arXiv:1204.4945 [hep-lat]].
 - [19] H. Ohno *et al.* [WHOT-QCD Collaboration], Phys. Rev. D **84**, 094504 (2011) [arXiv:1104.3384 [hep-lat]].
 - [20] H. T. Ding, EPJ Web Conf. **36**, 00008 (2012) [arXiv:1207.5187 [hep-lat]].
 - [21] O. Kaczmarek, Nucl. Phys. A **910-911**, 98 (2013) [arXiv:1208.4075 [hep-lat]].
 - [22] P. de Forcrand *et al.* [QCD-TARO Collaboration], Phys. Rev. D **63**, 054501 (2001) [hep-lat/0008005].
 - [23] N. Brambilla, A. Pineda, J. Soto, and A. Vairo, Nucl. Phys., B **566**, 275 (2000) [hep-ph/9907240].
 - [24] N. Brambilla, A. Pineda, J. Soto, and A. Vairo, Rev. Mod. Phys. **77**, 1423 (2005) [hep-ph/0410047].
 - [25] W. E. Caswell and G. P. Lepage, Phys. Lett. B **167**, 437 (1986).
 - [26] B. A. Thacker and G. P. Lepage, Phys. Rev. D **43**, 196 (1991).
 - [27] G. T. Bodwin, E. Braaten and G. P. Lepage, Phys. Rev. D **51**, 1125 (1995) [hep-ph/9407339].
 - [28] M. Laine, O. Philipsen, P. Romatschke, and M. Tassler, JHEP **03**, 054 (2007) [hep-ph/0611300].
 - [29] P. Petreczky, C. Miao and A. Mocsy, Nucl. Phys. A **855**, 125 (2011) [arXiv:1012.4433 [hep-ph]].
 - [30] M. Margotta, K. McCarty, C. McGahan, M. Strickland and D. Yager-Elorriaga, Phys. Rev. D **83**, 105019 (2011) [arXiv:1101.4651 [hep-ph]].
 - [31] A. Rothkopf, T. Hatsuda and S. Sasaki, Phys. Rev. Lett. **108**, 162001 (2012).
 - [32] Y. Burnier and A. Rothkopf, Phys. Rev. D **86**, 051503 (2012) [arXiv:1108.1579 [hep-lat]].
 - [33] Y. Burnier, M. Laine and M. Vepsalainen, JHEP **0801**, 043 (2008) [arXiv:0711.1743 [hep-ph]].
 - [34] M. Laine, O. Philipsen, and M. Tassler, JHEP. **09**, 066 (2007) [arXiv:0707.2458 [hep-lat]].
 - [35] A. Beraudo, J. P. Blaizot, and C. Ratti, Nucl. Phys. A **806**, 312 (2008) [arXiv:0712.4394 [nucl-th]].
 - [36] N. Brambilla, M. A. Escobedo, J. Ghiglieri, J. Soto and A. Vairo, JHEP **1009**, 038 (2010) [arXiv:1007.4156 [hep-ph]].
 - [37] L. Grandchamp, S. Lumpkins, D. Sun, H. van Hees and R. Rapp Phys.Rev. C **73**, 064906 (2006) [hep-ph/0507314].

- [38] F. Riek and R. Rapp, New J. Phys. **13**, 045007 (2011) [arXiv:1012.0019 [nucl-th]].
- [39] A. Emerick, X. Zhao and R. Rapp, Eur. Phys. J. A **48**, 72 (2012) [arXiv:1111.6537 [hep-ph]].
- [40] X. Zhao and R. Rapp, Nucl. Phys. A **859**, 114 (2011) [arXiv:1102.2194 [hep-ph]].
- [41] Y. Akamatsu and A. Rothkopf, Phys. Rev. D **85**, 105011 (2012) [arXiv:1110.1203 [hep-ph]].
- [42] M. C. Chu and T. Matsui, Phys. Rev. D **39**, 1892 (1989).
- [43] M. G. Mustafa, M. H. Thoma and P. Chakraborty, Phys. Rev. C **71**, 017901 (2005) [hep-ph/0403279].
- [44] N. Armesto *et al.*, J. Phys. G **35**, 054001 (2008) [arXiv:0711.0974 [hep-ph]].
- [45] J. Ruppert and B. Muller, Phys. Lett. B **618**, 123 (2005) [hep-ph/0503158].
- [46] P. Chakraborty, M. G. Mustafa and M. H. Thoma, Phys. Rev. D **74**, 094002 (2006) [hep-ph/0606316].
- [47] P. Chakraborty, M. G. Mustafa, R. Ray and M. H. Thoma, J. Phys. G **34**, 2141 (2007) [arXiv:0705.1447 [hep-ph]].
- [48] B. F. Jiang and J. R. Li, Nucl. Phys. A **832**, 100 (2010).
- [49] M. A. Escobedo, J. Soto and M. Mannarelli, Phys. Rev. D **84**, 016008 (2011) [arXiv:1105.1249 [hep-ph]].
- [50] M. A. Escobedo, F. Giannuzzi, M. Mannarelli and J. Soto, Phys. Rev. D **87**, 114005 (2013) [arXiv:1304.4087 [hep-ph]].
- [51] T. Song, Y. Park, S. H. Lee and C. Y. Wong, Phys. Lett. B **659**, 621 (2008) [arXiv:0709.0794 [hep-ph]].
- [52] H. Liu, K. Rajagopal and U. A. Wiedemann, Phys. Rev. Lett. **98**, 182301 (2007) [hep-ph/0607062].
- [53] M. Chernicoff, J. A. Garcia and A. Guijosa, JHEP **0609**, 068 (2006) [hep-th/0607089].
- [54] S. D. Avramis, K. Sfetsos and D. Zoakos, Phys. Rev. D **75**, 025009 (2007) [hep-th/0609079].
- [55] H. Liu, K. Rajagopal and U. A. Wiedemann, JHEP **0703**, 066 (2007) [hep-ph/0612168].
- [56] E. Caceres, M. Natsuume and T. Okamura, JHEP **0610**, 011 (2006) [hep-th/0607233].
- [57] Y. Liu, N. Xu and P. Zhuang, Phys. Lett. B **724**, 73 (2013) [arXiv:1210.7449 [nucl-th]].
- [58] S. Chakraborty and N. Haque, Nucl. Phys. B **874**, 821 (2013) [arXiv:1212.2769 [hep-th]].
- [59] M. Ali-Akbari, D. Giataganas and Z. Rezaei, Phys. Rev. D **90**, no. 8, 086001 (2014) [arXiv:1406.1994 [hep-th]].
- [60] B. K. Patra, H. Khanchandani and L. Thakur, Phys. Rev. D **92**, no. 8, 085034 (2015) [arXiv:1504.05396 [hep-th]].
- [61] A. Dumitru, Y. Guo and M. Strickland, Phys. Rev. D **79**, 114003 (2009) [arXiv:0903.4703 [hep-ph]].
- [62] A. Dumitru, Prog. Theor. Phys. Suppl. **187**, 87 (2011) [arXiv:1010.5218 [hep-ph]].
- [63] A. Dumitru, Y. Guo and M. Strickland, Phys. Lett. B **662**, 37 (2008) [arXiv:0711.4722 [hep-ph]].
- [64] F. Karsch, J. Phys. Conf. Ser. **46**, 122 (2006) [hep-lat/0608003].
- [65] O. Kaczmarek, F. Karsch, F. Zantow and P. Petreczky, Phys. Rev. D **70**, 074505 (2004) [hep-lat/0406036].
- [66] A. Dumitru, J. Lenaghan and R. D. Pisarski, Phys. Rev. D **71**, 074004 (2005) [hep-ph/0410294].
- [67] A. Dumitru, Y. Hatta, J. Lenaghan, K. Orginos and R. D. Pisarski, Phys. Rev. D **70**, 034511 (2004) [hep-th/0311223].
- [68] M. Cheng *et al.*, Phys. Rev. D **78**, 034506 (2008) [arXiv:0806.3264 [hep-lat]].
- [69] Y. Maezawa *et al.* [WHOT-QCD Collaboration], Phys. Rev. D **75**, 074501 (2007) [hep-lat/0702004].
- [70] O. Andreev and V. I. Zakharov, Phys. Lett. B **645**, 437 (2007) [hep-ph/0607026].
- [71] V. Agotiya, V. Chandra and B. K. Patra, Phys. Rev. C **80**, 025210 (2009) [arXiv:0808.2699 [hep-ph]].
- [72] L. Thakur, N. Haque, U. Kakade and B. K. Patra, Phys. Rev. D **88**, 054022 (2013) [arXiv:1212.2803 [hep-ph]].
- [73] L. Thakur, U. Kakade and B. K. Patra, Phys. Rev. D **89**, 094020 (2014) [arXiv:1401.0172 [hep-ph]].
- [74] S. Gao, B. Liu and W. Q. Chao, Phys. Lett. B **378**, 23 (1996).
- [75] B. Liu, P. N. Shen and H. C. Chiang, Phys. Rev. C **55**, 3021 (1997).
- [76] J. Takahashi, K. Nagata, T. Saito, A. Nakamura, T. Sasaki, H. Kouno and M. Yahiro, Phys. Rev. D **88**, 114504 (2013) [arXiv:1308.2489 [hep-lat]].
- [77] U. Kakade and B. K. Patra, Phys. Rev. C **92**, no. 2, 024901 (2015) [arXiv:1503.08149 [hep-ph]].
- [78] H. A. Weldon, Phys. Rev. D **26**, 1394 (1982).
- [79] M. E. Carrington, D. f. Hou and M. H. Thoma, Eur. Phys. J. C **7**, 347 (1999) [hep-ph/9708363].
- [80] N. Haque, A. Bandyopadhyay, J. O. Andersen, M. G. Mustafa, M. Strickland and N. Su, JHEP **1405**, 027 (2014) [arXiv:1402.6907 [hep-ph]].
- [81] J. I. Kapusta and C. Gale, "Finite-temperature field theory: Principles and applications(Cambridge University Press, Cambridge, England, 1996), 2nd ed.
- [82] O. Kaczmarek, F. Karsch, P. Petreczky and F. Zantow, Phys. Lett. B **543**, 41 (2002) [hep-lat/0207002].

- [83] A. Dumitru, Y. Guo, A. Mocsy and M. Strickland, Phys. Rev. D **79**, 054019 (2009) [arXiv:0901.1998 [hep-ph]].
- [84] K. A. Olive *et al.* [Particle Data Group Collaboration], Chin. Phys. C **38**, 090001 (2014).
- [85] M. Beneke and V. A. Smirnov, Nucl. Phys. B **522**, 321 (1998) [hep-ph/9711391].